Published in final edited form as:

Cell Rep. 2023 March 28; 42(3): 112264. doi:10.1016/j.celrep.2023.112264.

The conserved histone chaperone Spt6 is strongly required for DNA replication and genome stability

Catherine L.W. Miller[1,2,3], **Fred Winston**[1,4,*]

[1]Department of Genetics, Blavatnik Institute, Harvard Medical School, Boston, MA 02115, USA

[2]Department of Molecular and Cellular Biology, Harvard University, Cambridge, MA 02138, USA

[3]Present address: Laboratory of Genome Maintenance, Rockefeller University, New York, NY 10065, USA

[4]Lead contact

SUMMARY

Histone chaperones are an important class of proteins that regulate chromatin accessibility for DNA-templated processes. Spt6 is a conserved histone chaperone and key regulator of transcription and chromatin structure. However, its functions outside of these roles have been little explored. In this work, we demonstrate a requirement for *S. cerevisiae* Spt6 in DNA replication and, more broadly, as a regulator of genome stability. Depletion or mutation of Spt6 impairs DNA replication *in vivo*. Additionally, *spt6* mutants are sensitive to DNA replication stress-inducing agents. Interestingly, this sensitivity is independent of the association of Spt6 with RNA polymerase II (RNAPII), suggesting that *spt6* mutants have a transcription-independent impairment of DNA replication. Specifically, genomic studies reveal that *spt6* mutants have decreased loading of the MCM replicative helicase at replication origins, suggesting that Spt6 promotes origin licensing. Our results identify Spt6 as a regulator of genome stability, at least in part through a role in DNA replication.

In brief

Spt6 has been primarily studied for its roles during transcription. Miller and Winston show that it also has a role in DNA replication. They demonstrate that *spt6* mutants are defective for replication *in vivo*, at least in part by defects in loading the MCM helicase complex, which is required for origin firing.

*Correspondence: winston@genetics.med.harvard.edu.

AUTHOR CONTRIBUTIONS

C.L.W.M. and F.W. designed the experiments. C.L.W.M. performed all experiments. C.L.W.M. and F.W. wrote the manuscript.

SUPPLEMENTAL INFORMATION

Supplemental information can be found online at https://doi.org/10.1016/j.celrep.2023.112264.

DECLARATION OF INTERESTS

The authors have no competing interests.

INCLUSION AND DIVERSITY

We support inclusive, diverse, and equitable conduct of research.

Graphical Abstract

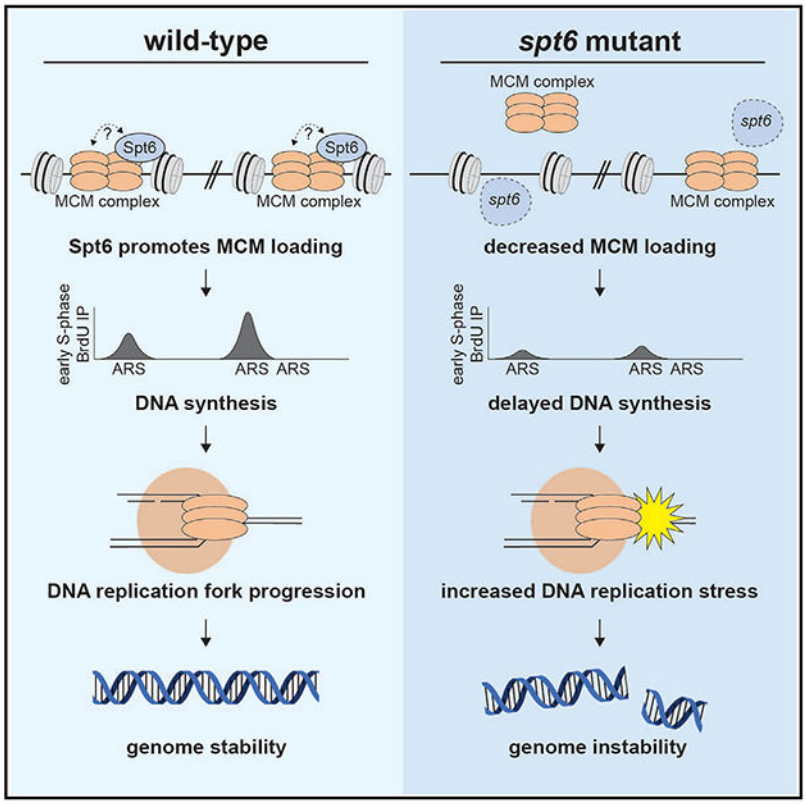

INTRODUCTION

Histone chaperones are conserved eukaryotic proteins that directly regulate histone-DNA interactions to enable transcription, DNA replication, and DNA repair.[1,2] They function in cooperation with histone-modifying enzymes and chromatin remodelers to coordinate the dynamic opening of chromatin to allow DNA-templated activities while also modulating the closing of chromatin to prevent the loss of nucleosomes and genome integrity. Insights into the functions of histone chaperones are important to understand chromatin-regulated processes as well as how mutations that alter histones and histone chaperones contribute to cancer and other human diseases.[3–5]

Spt6 is a highly conserved histone chaperone of great biological importance. It is essential for viability in *S. cerevisiae*,[6,7] and it is required for proper development in *C. elegans*,[8] zebra-fish,[9,10] and *Drosophila*.[11,12] In mammalian systems, Spt6 is required for embryonic stem cell maintenance, muscle cell differentiation, epithelial cell differentiation, and immunoglobulin class-switch recombination.[13–17] Additionally, loss-of-function alleles of the human homolog *SUPT6H* are greatly underrepresented,[18] indicating that it is likely essential in humans.

Spt6 is a large multi-domain protein that is a vital component of the transcription elongation complex.[19–22] The C-terminal tandem SH2 domains of Spt6 directly interact

with phosphorylated residues in the C-terminal domain (CTD) and linker region of Rpb1, the largest subunit of RNA polymerase II (RNAPII).[23–27] Furthermore, Spt6 directly interacts with histones and nucleosomes and can assemble nucleosomes *in vitro*.[28–32] As such, Spt6 plays critical roles regulating transcription initiation,[33,34] elongation,[12,35–37] repression of intragenic transcription,[38–42] and termination.[36,43,44] At transcribed genes, Spt6 is required to establish and/or maintain nucleosome positioning[28,34,39,45–48] as well as for certain histone modifications, including methylation of H3K4,[17,46,49,50] H3K27,[13,15,51] and H3K36.[46,52–55] Combined, these works demonstrate the important roles Spt6 plays in regulating eukaryotic transcription. However, the roles of Spt6 outside of transcription remain poorly understood.

Several lines of evidence have hinted that Spt6 may also have a role in DNA replication. Yeast *spt6* mutants have phenotypes consistent with DNA replication defects, such as an increase in recombination frequency,[56,57] chromosome segregation errors,[58] and sensitivity to the DNA replication inhibitor hydroxyurea (HU).[59,60] Consistent with this potential role, depletion of Spt6 from mammalian cells decreases total DNA synthesis.[36] Outside of this result, no studies have been performed to address if and how Spt6 might be required for DNA replication.

In this study, we provide evidence that Spt6 has a critical role in DNA replication in *S. cerevisiae*. First, DNA replication is impaired *in vivo* either after Spt6 depletion or in *spt6* mutants. In addition, *spt6* mutants have several phenotypes common to replication mutants, including sensitivity to DNA-damaging agents, an increased level of DNA double-strand breaks, and enhanced growth defects when combined with the loss of the DNA replication factor Ctf4 or with the loss of DNA replication checkpoints. Furthermore, Spt6 is required for origin licensing, as the association of the MCM helicase with replication origins is severely decreased in *spt6* mutants. Finally, our results suggest that RNA-DNA hybrids are not driving the genome instability observed in *spt6* mutants, as RNA-DNA hybrid levels are not elevated in *spt6* mutants. Taken together, these results demonstrate the importance of Spt6 in DNA replication and, as a consequence, for genome stability.

RESULTS

Spt6 depletion causes DNA replication defects

To examine the requirement for Spt6 in DNA replication, we first tested whether loss of Spt6 impaired DNA replication *in vivo*. As Spt6 is essential for viability in *S. cerevisiae*, yeast strains were constructed in which we could deplete Spt6 using an auxin-inducible degron (AID) system[39,61] and then assay the level of newly synthesized DNA by measuring the incorporation of the thymidine analog BrdU.[62,63] We synchronized cells in G1 with the yeast mating pheromone α-factor, followed by treatment with the auxin indole-acetic acid (IAA) for 60 min to deplete Spt6-AID, or with DMSO as a non-depletion control (Figure 1A). In the depleted samples, Spt6 protein levels were reduced to ~10% of non-depleted levels, and cells remained arrested in G1 following depletion (Figures S1A and S1B). Importantly, cell viability was greater than 88% in all Spt6-depleted samples. After release from α-factor arrest, samples were harvested at an early time point in S phase (30 min). Newly replicated DNA was isolated by immunoprecipitation with an anti-BrdU antibody,

followed by qPCR at well-characterized early and late yeast replication origins (ARSs). For normalization between samples, an equal amount of BrdU-labeled *S. pombe* genomic DNA was spiked into each sample prior to immunoprecipitation.

Our results showed a requirement for Spt6 for DNA synthesis. In the non-depleted samples, there was a high level of BrdU incorporation at the early replication origin *ARS1* but not at the late-firing origin *ARS301*, as expected. In contrast, in the Spt6-depleted samples, BrdU incorporation was undetectable at either origin (Figure 1B). These results are in agreement with recent work in mammalian cells where depletion of Spt6 also resulted in loss of BrdU incorporation.[36]

To test whether the Spt6-depleted cells had arrested growth rather than impaired DNA synthesis, we also assayed S-phase progression following Spt6 depletion by monitoring total DNA content by flow cytometry (Figure 1C). Our results showed that Spt6-depleted cells completed S phase but with a delay in DNA synthesis (Figure 1D). The median fluorescence value for non-depleted samples at 30 min was similar to the median fluorescence value for Spt6-depleted cells at 45 min. By 75 min, the Spt6-depleted cells had completed DNA synthesis, showing that cells were capable of completing at least one cell cycle in the absence of Spt6. These data indicate that Spt6 has a role in DNA replication.

spt6 mutants are sensitive to chemicals that cause DNA replication stress, and they have elevated DNA double-strand breaks

To investigate the requirement for Spt6 in DNA replication in greater depth, we analyzed *spt6* mutants. The *spt6* mutants provide the opportunity to analyze DNA replication when Spt6 is impaired during continuous cell division at 30°C, in contrast to Spt6 depletion, which eventually leads to inviability. For these experiments, we chose four *spt6* mutations (Figure 2A): (1) *spt6-YW*,[59,60] (2) *spt6-140*[57,64] (3) *spt6-1004*,[38,39] and (4) *spt6-50*.[59] For each allele, the Spt6 mutant proteins are present at near wild-type levels during growth at 30°C (Figure S2A). Previous studies and this work show that these mutations cause distinct phenotypes with respect to transcription, histone modifications, RNAPII binding, and nucleosome organization[39,53,60,65,66] (Figures 2A, S2B, and S2C).

As a first step to understand if these *spt6* mutants have defects in DNA replication, we tested their sensitivity to agents that induce DNA replication stress, including HU, phleomycin, and methyl methanesulfonate. Our results showed sensitivities to all of these agents, in agreement with previous reports.[60,65] Our analysis also showed allele specificity, as *spt6-YW* and *spt6-50* were the most sensitive (Figure 2B; Table S1).

One consequence of increased replication stress is the formation of DNA double-strand breaks (DSBs).[67] DSBs formed during S phase are primarily repaired by the homologous recombination (HR) pathway.[68] As *spt6* mutants had sensitivities associated with replication stress and, as shown later, showed a dependence on S-phase checkpoints, we hypothesized that they may also have elevated levels of DSBs.

To measure the level of DSBs, we took advantage of the observation that DSBs can be assayed by the presence of Rad52-YFP foci.[69] In yeast, Rad52 is a critical component of

the HR repair pathway. Our results showed that *spt6* mutants have an increased level of Rad52-YFP foci, ranging from a modest effect for *spt6-YW* to a large increase for *spt6-50*. Thus, *spt6* mutants have an elevated level of DSBs (Figure 2C).

Evidence that the DNA replication stress phenotypes of *spt6-50* and *spt6-YW* are independent of transcription

The *spt6-50* mutation causes loss of the C-terminal SH2 domains, which were previously shown to be necessary for the association of Spt6 with Rpb1, the largest subunit of RNAPII.[23–27] The greatly reduced Spt6-Rpb1 interaction in *spt6-50* (Figure S2C) provided an opportunity to test whether the sensitivity of *spt6-50* to chemicals that cause replication stress is independent of the Spt6-Rpb1 interaction. To do this, we took advantage of a mutation in *RPB1, rpb1-FSP*, that also disrupts the Spt6-Rpb1 interaction in the presence of wild-type Spt6.[27] When we compared the *rpb1-FSP* mutant with *spt6-50*, as well as with *spt6-YW*, our results showed that only the *spt6* mutants were sensitive to chemicals that cause DNA replication stress (Figure 2D), in agreement with a previous study.[70] In contrast, as expected, both the *rpb1* and *spt6* mutants exhibited transcription defects, as measured by their Spt$^-$ phenotype (the ability to suppress the Lys$^-$ phenotype caused by the *lys2-1288* mutation [Figure 2D]). The broader phenotypes of the *spt6-50* mutant compared with *rpb1-FSP* support a role for Spt6 in both transcription and DNA replication.

Previous transcriptional studies of *spt6-YW* also suggested that its sensitivity to chemicals that cause replication stress, as well as the DNA replication defects shown later, is independent of transcription. During growth at 30°C, *spt6-YW* mutants did not have major changes in mRNA levels, including for genes encoding the G1 cyclins, DNA replication machinery, or ribonucleotide reductase (Figures S2D and S2E) (data available at GEO: GSE160821[60]). Therefore, for the *spt6-YW* mutant, any defects in DNA replication are unlikely to be the consequence of transcriptional changes.

spt6 mutants have negative genetic interactions with DNA replication-associated factors

To test for genetic evidence for a role for Spt6 in DNA replication, we analyzed *spt6* mutants with respect to altered growth in combination with different classes of mutations that cause replication stress. For these experiments, we focused on the *spt6-YW* and *spt6-50* mutants, given their extreme sensitivity to chemicals that cause replication stress. First, we hypothesized that if Spt6 is involved in DNA replication, *spt6* mutants would exhibit growth defects in combination with replisome mutants such as Ctf4, an important but non-essential member of the DNA replication machinery. Ctf4 acts as a structural hub within the replisome to coordinate DNA replication.[71–74] We found that, compared with each single mutant, the *spt6-YW ctf4Δ* and *spt6-50 ctf4Δ* double mutants had increased growth defects under permissive growth conditions and were extremely sensitive to low doses of DNA replication stress-inducing agents (Figures 3A and 3B; Table S1). The severe growth defects of *spt6* mutants in combination with loss of a DNA replication factor provide additional evidence that Spt6 is involved in DNA replication.

Second, if *spt6* mutants impair DNA replication, we expected that they would have an increased reliance on S-phase checkpoint factors. There are two main branches of the yeast

S-phase checkpoint. One branch responds to DNA damage, mediated by Rad9, while an alternate branch responds to stalled DNA replication forks, mediated by Mrc1.[75] Our results showed that both *spt6-YW* and *spt6-50* caused increased sensitivity to treatments that induce S-phase checkpoint activation when combined with *mrc1Δ* (Figures 3C and 3D; Table S1). We observed milder effects when *spt6* mutants were combined with *rad9Δ*, as only *spt6-50 rad9Δ* double mutants had synthetic growth defects (Figure 3E; Table S1). As a control, we also combined *spt6* mutations with *mad2Δ*; Mad2 is a spindle-assembly checkpoint factor.[76] We observed no genetic interactions for these double mutants under the same conditions (Table S1). The strong negative genetic interactions of *spt6* mutations with *mrc1Δ* suggest that stalled DNA replication forks are particularly difficult for *spt6* mutants to overcome in the absence of this S-phase checkpoint.

Given the elevated level of Rad52-YFP foci, we also tested for genetic interactions between *spt6* mutations and a deletion of *RAD52*. Our results showed a mild growth defect for both *spt6-YW rad52Δ* and *spt6-50 rad52Δ* double mutants compared with the single mutants at permissive and elevated temperatures (Table S1). These growth defects were exacerbated when the cells were treated with drugs that induce replication stress. In contrast, we observed no growth effects when *spt6* mutants were combined with a deletion of *LIG4*, a member of the non-homologous end joining pathway (Table S1). This suggests that the increased level of DSBs in *spt6* mutants makes the cells more dependent on homologous recombination.

spt6 mutants have S-phase progression defects

As we had observed a delayed S-phase progression after Spt6 depletion, we asked whether this delay was also present in *spt6* mutants. Similar to our previous experiments, we synchronized cells in G1, released them into fresh medium, and harvested samples throughout one 90 min cell cycle for analysis of total DNA content by flow cytometry (Figure 4A). From these results, we observed an increase in DNA content over time in wild-type cells that follows the well-defined timing of the yeast cell cycle. However, both the *spt6-YW* and *spt6-50* mutants exhibited a delay in DNA synthesis compared with wild type, which was apparent from the shift in the curve of median fluorescent intensity values (Figure 4B). This delay was also apparent by plotting the distribution at 30 min, when cells are in early S phase, where we observed an increased number of cells between 1N and 2N content for both mutants, similar to what we observed after Spt6 depletion (Figure 4C). Combined, our results showed that loss or impairment of Spt6 function causes DNA replication defects.

spt6 mutants have DNA replication initiation defects *in vivo*

We hypothesized that DNA replication could be impaired by several different mechanisms in *spt6* mutants. Among these possibilities, we considered a requirement for Spt6 for a normal level of initiation or elongation by DNA polymerases, similar to how Spt6 regulates initiation and elongation of RNAPs.[12,33–37,39] In this general model, the impairment in *spt6* mutants would decrease the level of DNA synthesis around known origins. We also considered the possibility that Spt6 controls the fidelity of DNA replication initiation, similar to how Spt6 prevents intragenic initiation of transcription from within gene

bodies.[38–42,46,60] By this model, Spt6 impairment would result in the initiation of replication from ectopic or dormant sites, thereby diluting replication factors and reducing the overall level of functional replication.

To begin to differentiate between these possibilities, we measured the level and genomic location of newly synthesized DNA by measuring BrdU incorporation in wild-type and *spt6* mutant strains. Cells were first synchronized in G1 by treatment with α-factor and then released into medium containing 0.2 M HU and BrdU for 1 h, resulting in arrest in early S phase (Figure 4D). After the HU arrest, DNA was extracted, BrdU-labeled DNA was immunoprecipitated, and next-generation sequencing libraries were prepared. For normalization between libraries, we used a spike-in control of BrdU-labeled *S. pombe* DNA. Biological duplicates were performed for each strain, and the replicates correlated well, with Pearson correlations for spike-in normalized immunoprecipitation (IP) signals at all loci ranging from 0.93 to 0.99 (Figure S3A). Importantly, we showed that the 1 h treatment with 0.2 M HU did not greatly affect *spt6* mutant cell viability despite the HU sensitivity of these mutants when grown on plates (wild type: 91%–100%, *spt6-YW*: 77%–93%, and *spt6-50*: 72%–99% viability). We also note that, for reasons we do not understand, the integration of the genes necessary for BrdU uptake and incorporation (hENT1 and HSV-1 TK[62]) caused a growth defect specifically in *spt6-50* strains, increasing their generation time from 2.5 to 3.8 h (compared with 1.5 h for wild type). We also assayed global BrdU incorporation, comparing wild type with the two *spt6* mutants in G2-arrested cells in which DNA synthesis should be complete. While *spt6-YW* has approximately the same incorporation, *spt6-50* has a reduced level, consistent with its growth defect when it contains the genes enabling BrdU uptake (Figure S3B).

To analyze our results, we first plotted the spike-in normalized BrdU-IP signal for wild type and *spt6* mutants at a set of 228 high-confidence *S. cerevisiae* replication origins.[77–79] For the wild-type strain, BrdU incorporation occurred at a subset of the origins, as expected for early-S-phase-arrested cells (Figure 4D). These were primarily early origins based on previously reported replication timing information[80] (Figure S3C). For the two *spt6* mutants, we observed a striking decrease in the number of origins that were activated in HU-arrested cells as well as in the level of BrdU incorporation at those origins, with incorporation in the *spt6-50* mutant barely detectable (Figure 4D).

To specifically identify which origins were activated across samples, we calculated the overlap between peaks of BrdU signal and the 228 origins (see STAR Methods). In wild-type cells, we identified BrdU incorporation at 97 origins. In contrast, we detected only 50 and 37 origins in *spt6-YW* and *spt6-50*, respectively. An example of origins that are activated compared with the BrdU-IP signal is shown for chromosome VII, one of the largest chromosomes (Figure 4E). All but one detected origin in each *spt6* mutant was in the subset of the 97 origins identified in wild-type cells (Figure S3E). Our results indicate that after HU arrest, only a subset of origins are activated in each of the *spt6* mutants, with the level of activation generally less than in wild type.

As HU treatment might confound our analysis by inducing replication stress or by reducing the level of RNAPII on chromatin,[81] we repeated our BrdU-IP without HU treatment.

Instead, we released α-factor-synchronized cells into fresh medium and harvested cells after 30 min (Figure 4F). Based on flow cytometry data, this time point represents early-S-phase cells, similar to the block imposed by HU. Again, duplicate biological replicates were collected, and they correlated well, with the Pearson correlations for spike-in normalized IP signals at all loci ranging from 0.86 to 0.98 (Figure S3D).

Our results from these samples were similar to our results from the HU-treated samples in that many fewer origins were activated in *spt6* mutants compared with wild type (Figures 4F and 4G). In the early-S-phase wild-type samples, we identified 114 origins. We identified 45 origins in *spt6-YW* and 12 origins in *spt6-50*, which were largely a subset of peaks observed in wild-type samples (Figures 4F, 4G, and S3E). Similar to our HU results, we again observed a dramatic reduction in signal at origins in both *spt6-YW* and *spt6-50* (Figures 4F and 4G).

As we did not observe aberrant activation of late-firing origins in *spt6* mutants, nor did we observe significant signals at non-origin regions (Figure 4; data not shown), we conclude that *spt6* mutants do not regulate DNA replication initiation fidelity. Rather, our data suggest that initiation and/or elongation is impaired at early replication origins in *spt6* mutants.

Spt6 promotes origin licensing

To test directly whether Spt6 plays a role in DNA replication initiation, we assayed the genomic localization of the MCM complex, a helicase essential for DNA replication that is loaded at all origins as cells enter G1, a process known as origin licensing.[82] If *spt6* mutants impair the association of the MCM complex with origins, this would strongly support a requirement for Spt6 at an essential step in the initiation of DNA replication.

To assay MCM localization, we performed chromatin IP followed by sequencing (ChIP-seq) of the MCM complex in α-factor-arrested cells. Briefly, cells were α-factor arrested, chromatin was isolated, and IP was performed using native antisera targeting the MCM2-7 complex. For normalization between sequencing libraries, we used a spike-in control of *S. pombe* chromatin. Each strain was analyzed in three or four biological replicates, and the replicates correlated well, with Pearson correlations for spike-in normalized IP/input signals ranging from 0.70 to 0.94 (Figure S4A).

We analyzed our results in terms of the peaks identified in each strain as well as for the level of occupancy at each peak. Overall, our results showed that the *spt6* mutants had a striking decrease in MCM occupancy (Figure 5). First, we identified reproducible peak regions genome-wide. We detected 235, 142, and 202 peaks for wild type, *spt6-YW*, and *spt6-50* respectively (Figure S4B). Over 80% of peaks identified in wild-type cells were also detected in *spt6* mutants. Furthermore, there is a strong overlap between detected peaks and known replication origins. These data indicate that MCM positioning is not altered in *spt6* mutants.

Second, we compared the spike-in normalized occupancy of MCM at each of the 235 identified wild-type peak regions (Figure 5A) and at high-confidence origins (Figures 5B and 5C). *spt6* mutants had a significant decrease in MCM occupancy at peak regions

(Figures S4C and S4D). These results indicate that Spt6 promotes origin licensing at or before MCM loading.

Spt6 may physically interact with the DNA replication machinery

If Spt6 functions directly in DNA replication, we might be able to detect a physical interaction between Spt6 and the DNA replication machinery. Therefore, we assayed for an Spt6-MCM interaction by co-immunoprecipitation experiments. As described below, while our results showed that Spt6 and MCM physically interact in cell extracts, the results do not allow us to conclude that this interaction occurs specifically during DNA replication.

First, in asynchronous cells, we observed co-immunoprecipitation between wild-type Spt6 and both Mcm4 (Figures 6A, lanes 4 and 6, 6B, and 6C) and Mcm2 (Figures S5A–S5C). The Spt6-Mcm co-immunoprecipitations were largely resistant to treatment with the endonuclease benzonase (Figures S5A–S5C), suggesting that the interactions were not caused by DNA-mediated interactions between two chromatin-associated factors. Furthermore, this interaction was stable when tested up to 1 M NaCl (Figure S5D). When we tested the *spt6* mutants, we found that the Spt6-Mcm4 co-immunoprecipitation was greatly decreased in *spt6-50* mutants, suggesting that the Spt6 SH2 domains are required for the Spt6-MCM interaction (Figures 6A–6C). In the *rpb1-FSP* mutant, in which Spt6 no longer co-immunoprecipitates with RNAPII, Spt6-MCM co-immunoprecipitation was still detected, albeit reduced (Figure S5E).

We then assayed Spt6-Mcm4 co-immunoprecipitation across the cell cycle by testing wild-type cells arrested in G1, in S phase, and in G2/M. We did not observe any cell-cycle dependence of the Spt6-Mcm4 interaction when we quantified the IP/input signal, despite seeing a reduced interaction in G1 phase (Figure 6D). Given previous evidence that Mcm proteins are cytoplasmic in G2/M[83–85] while Spt6 is nuclear,[86] the Spt6-Mcm4 interaction that we observed could reflect a fortuitous interaction of Spt6 and Mcm4 in cell extracts rather than a regulated interaction *in vivo*. To test this further, we assayed whether Spt6 and Mcm4 co-immunoprecipitate after mixing lysates in which only one of each pair is epitope tagged. In this case, we also observed co-immunoprecipitation (Figure S5F). Together, these results show that Spt6 and Mcm proteins interact, raising the possibility of a direct role for Spt6. However, we have as yet been unable to determine whether this interaction is relevant to the function of Spt6 during DNA replication.

Transcription also contributes to *spt6*-mediated genome instability

While our focus has been on Spt6 and DNA replication, previous studies also suggested that Spt6 regulates genome stability, at least in part, by transcription. Through its role in transcription, Spt6 has been shown to cause cell-cycle defects,[87] to regulate DSB repair in cancer cells,[88] and to lead to the accumulation of harmful RNA-DNA hybrids at non-coding RNA loci.[43] Given that both DNA replication and transcription can independently lead to genome instability,[89] we addressed whether replication and/or transcription was the underlying cause of a particular aspect of Spt6-associated genome instability, an elevated level of recombination.

We examined hyper-recombination in *spt6* mutants, as it was previously reported that an *spt6-140* mutant is hyper-recombinogenic.[56,57] Using a previously described recombination reporter system,[57] our results showed that all four *spt6* alleles caused increased levels of recombination compared with wild type (Figure 7A), from a 3-fold increase for *spt6-1004* to a 30-fold increase for *spt6-50*. Previous studies showed that a mutant in the histone chaperone FACT also caused a 3-fold increase in recombination frequency under similar conditions.[90] To test if transcription contributes to the hyper-recombination phenotype, we used a second reporter that contains a transcription terminator that prevents transcription across the reporter locus (Figures 7B and S6).[57] Our results showed that inhibiting transcription reduces, but does not abolish, the hyper-recombination phenotype for the *spt6-140* and *spt6-50* mutants. This indicates that both transcription-dependent and -independent defects contribute to Spt6-mediated hyper-recombination in *spt6* mutants.

R-loops are not a major contributor to *spt6*-mediated genome instability

Next, we asked if R-loops are elevated in yeast *spt6* mutants, as a recent study showed that human Spt6 controls R-loop levels over some non-coding regions.[43] R-loops are transcription-dependent nucleic acid structures that consist of an RNA-DNA hybrid and an extruded single-stranded DNA loop. They have both regulatory and toxic effects on cells and have been the focus of many recent studies.[91–94]

If increased RNA-DNA hybrid formation in *spt6* mutants contributed to genome instability phenotypes, we would expect that altering RNA-DNA hybrid levels might enhance or suppress *spt6* mutant phenotypes. To test this, we manipulated the levels of the RNA-DNA hybrid-specific endoribonuclease RNaseH in our mutants. First, we combined each of the four *spt6* mutations with deletion mutations of the genes encoding the two yeast RNaseH enzymes, *RNH1* and *RNH201*. In these mutants, RNA-DNA hybrid levels are greatly increased.[95] Our results showed no change in the *spt6* phenotypes, suggesting that increasing RNA-DNA hybrid levels does not exacerbate the *spt6* genome instability phenotypes (Table S1). Next, we tested whether reducing RNA-DNA hybrid levels by overexpression of *RNH1* would suppress hyper-recombination. We found that overexpression of *RNH1* did not reduce the recombination frequency compared with expression of an empty vector control in *spt6-YW, spt6-140*, or *spt6-1004* strains (Figure 7C). The *spt6-50* mutant had more variable results, although there was no statistical difference compared with wild type.

Finally, we measured the level of RNA-DNA hybrids in two *spt6* mutants using DNA-RNA hybrid IP (DRIP) (see STAR Methods). Genome-wide experiments in *spt6-YW* indicated that the level of RNA-DNA hybrids is decreased compared with wild type. We note that there was no spike-in to normalize for the genome-wide data (Figure 7D). Therefore, we repeated these experiments adding exogenous spike-in *S. pombe* genomic DNA and assayed by DRIP-qPCR in both *spt6-YW and spt6-50* (Figure 7E). We observed variable RNA-DNA hybrid levels across two tested loci in wild-type samples compared with *spt6* mutants. However, we did not generally observe increased levels of RNA-DNA hybrids in *spt6* mutants. These findings are in agreement with reduced RNAPII occupancy in the *spt6-YW*

mutant.[60] In conclusion our results suggest that altered RNA-DNA hybrid levels do not cause the *spt6* genome instability phenotypes.

DISCUSSION

The results presented in this article provide strong evidence that Spt6, a histone chaperone previously shown to control transcription and chromatin structure, is also critically required for DNA replication, likely at the level of initiation. A functional requirement for Spt6 in DNA replication was demonstrated from the analysis of Spt6 depletion and of *spt6* mutants, both of which revealed a delayed S phase and reduced DNA synthesis from early origins of replication. The cause of these defects can be accounted for by the result that Spt6 is required for a normal level of association of the MCM complex with replication origins, as MCM association is required for origin licensing.[96–99] Supporting data also include extensive genetic analyses that showed the sensitivity of *spt6* mutants to DNA-damaging agents, as well as double-mutant analyses that indicated greatly enhanced mutant phenotypes when *spt6* mutations were combined with mutations that impair DNA replication factors, S-phase checkpoint regulators, and recombination factors. Taken together, these results suggest that Spt6, like some other histone chaperones, including Asf1[100] and FACT,[101] are required for both DNA replication and transcription.

While the precise function of Spt6 in DNA replication remains uncertain, our results have pointed to a role in origin licensing. While origins are nucleosome free, likely due to a combination of the AT-rich sequence and the nucleosome remodeling ability of ORC,[102] there are several aspects of chromatin structure that control initiation.[103] These include nucleosome positioning around origins,[104–107] histone modifications at replication origins,[108–110] and transcription across origins.[111–113] Given the multi-functional nature of Spt6 in chromatin and transcription, its requirement for the association of MCM with origins might be dependent upon these functions. However, under the permissive growth conditions of our experiments, nucleosome positioning, histone modifications, and transcription across origins are not strongly affected. This is particularly true for *spt6-YW* mutants, which have been extensively characterized.[60] Therefore, additional Spt6 functions must also be considered, such as possible direct interactions of Spt6 with the MCM complex, ORC, or other proteins involved in replication initiation.

Our BrdU-seq analysis showed that the defect in *spt6* mutants occurs by reduced synthesis from known origins. Before these experiments, we had considered the possibility that *spt6* mutants might allow ectopic synthesis from non-origin loci, given that these mutants also allow transcription initiation from intragenic promoters that are normally repressed. However, the fidelity of the initiation of replication is not detectably altered in the *spt6* mutants we have studied. This difference between replication and transcription may reflect the different sequence requirements for the two events, with less specific information required for the initiation of transcription versus the initiation of DNA replication, which is defined by the ARS sequence in *S. cerevisiae*.[79] It would be interesting to see if loss of Spt6 function resulted in cryptic replication in mammalian cells, where DNA origins are not defined by known DNA-binding motifs.[114]

Histone chaperones contribute to genome instability through a variety of different mechanisms. One mechanism that has been the focus of recent studies is the relationship between histone chaperones, such as FACT,[90,115] and R-loops. A recent study depleted Spt6 from mammalian cells and demonstrated that the abundant R-loop signatures at mRNA loci were decreased genome-wide, while the small proportion of R-loops present at non-coding loci increased.[43] These changes correlated with the level of transcription present at each transcription unit, as has been previously seen.[116] Our finding, that yeast *spt6* mutants do not have elevated levels of R-loops, agrees with this work. It further highlights that the replication stress observed in *spt6* mutants, or the depletion of Spt6 from mammalian cells, may be caused by a direct role of Spt6 in replication or a role for Spt6 in mediating transcription-replication conflicts.

As a protein required for both DNA replication and transcription, Spt6 may be required to resolve transcription-replication conflicts, either independently or as part of a histone chaperone network. Interestingly, a recent study showed that Spt2, another histone chaperone, is required to help resolve transcription-replication conflicts.[117] As the recruitment of Spt2 to chromatin is partially dependent upon Spt6,[118] this suggests one mechanism by which Spt6 might help to maintain genome stability. Another intriguing aspect of our results relates to the close functional connections between Spt6 and FACT,[30,40,45,60,119] an essential histone chaperone that functions in transcription and replication and mediates transcription-replication conflicts.[90,101,120] FACT may play a different role in replication than Spt6, as FACT appears to function at a post-initiation step.[121,122] However, the respective contributions of Spt6 and FACT to DNA replication and genome stability are interesting topics for future studies, especially as FACT emerges as a potential therapeutic target in cancer.[123]

In conclusion, our studies have unveiled a role for Spt6 in DNA replication. Further work is needed to define the precise function of Spt6 in replication and to continue to understand the connection between the roles of Spt6 in replication, transcription, and conflicts between the two. Future studies will benefit from the identification of *spt6* alleles that specifically impair replication and not transcription, as such alleles have been valuable in studies of both FACT[124] and another factor that controls both transcription and replication, Sen1.[125]

Limitations of the study

Our study reveals an import function of Spt6 in DNA replication. However, to fully demonstrate a role of Spt6 in DNA replication, *in vitro* DNA replication assays with purified components should be performed. Another limitation of our study is the growth defect that occurs in the *spt6-50* mutant when combined with BrdU incorporation components. This could lead us to overestimate the effect of the *spt6-50* mutant on DNA replication as measured by BrdU-IP. We note that the *spt6-50* mutant strains used in co-immunoprecipiation and ChIP experiments do not have this defect. Finally, while we have tried to separate the transcription and replication defects observed in *spt6* mutants, true separation of function alleles is still lacking and could further differentiate direct and indirect mutant phenotypes.

STAR★METHODS

RESOURCE AVAILABILITY

Lead contact—Further information and requests for resources and reagents should be directed to and will be fulfilled by the lead contact, Fred Winston (winston@genetics.med.harvard.edu).

Materials availability—The unique reagents generated in our study, yeast strains and plasmids, are available upon request without restriction.

Data and code availability

- Genome-wide sequencing data have been deposited at GEO and are publicly available as of the date of publication. Accession numbers are listed in the key resources table. All data reported in this paper will be shared by the lead contact upon request.
- All original code has been deposited at GitHub and is publicly available as of the date of publication. The DOI is listed in the key resources table.
- Any additional information required to reanalyze the data reported in this paper is available from the lead contact upon request.

EXPERIMENTAL MODEL AND SUBJECT DETAILS

Yeast strains and growth—All *S. cerevisiae* strains used in this study are in an S288C *GAL2* background. They were constructed by standard methods either by transformation, cross, or CRISPR-Cas9 mutagenesis.[131] All *S. cerevisiae* liquid cultures were grown in YPD (1% yeast extract, 2% peptone, 2% glucose) at 30°C unless otherwise mentioned. For spike-in normalization, *S. pombe* liquid cultures were grown in YES (0.5% yeast extract, 3% glucose, 225 mg/l each of adenine, histidine, leucine, uracil, and lysine) at 32°C.

METHOD DETAILS

Yeast dilution plating (spot tests)—Yeast strains were grown to saturation in liquid YPD and were then serially diluted 10-fold and plated onto the indicated media: YPD 30°C (permissive), YPD 37°C (high temperature), hydroxyurea (HU), phleomycin, methyl methanesulfonate (MMS), ultra-violet light (UV), or SC-Lys. Plates were incubated for three days. All experiments were performed at least in duplicate. Each plate contained a wild-type and single mutant control, although only one representative example of these controls is shown.

Recombination assays—Recombination frequency reporters were previously described.[57] Recombination frequencies were determined as the average frequency of six independent colonies. For each strain, two independent experiments were performed, for a total of 12 independent colonies per strain. For each colony, strains were plated on SC complete to determine cell viability and SC-His to determine His^+ recombinants. Recombination frequencies are reported as the ratio of these two values. Yeast *RNH1* was cloned into pRS414 under the expression of an estradiol-inducible promoter (pKW26).

Strains expressing the Z3EV activator were transformed with pRS414 or pKW26, and grown under selective conditions SC-Trp. RNaseH overexpression was induced by addition of estrodiol overnight. Recombination frequencies were determined as described above, except only six colonies were assayed per genotype.

DNA-RNA IP (DRIP)—Yeast strains were harvested during mid-log phase (OD~0.6). For DRIP-seq, genomic DNA was isolated using Qiagen Tip kit according to manufacturer's protocol with the exception that RNase was not added to buffer G2. Genomic DNA was first treated with S1 nuclease for 30 minutes at 50°C (as described in [95]). Samples were then fragmented by sonication to ~300 bp. For qPCR analysis, genomic DNA was isolated by phenol:chromoform extract followed by a brief treatment with RNaseA/T1 in 300 mM NaCl. DNA was fragmented by overnight digestion at 37°C with restriction enzymes (AccI, EcoRV, NcoI, HaeIII, BsrG1) in cutsmart buffer in the presence or absence of 20 U RNaseH. For DRIP-seq and DRIP-qPCR, following fragmentation, samples were purified by phenol:chloroform extraction then ethanol precipitated. Samples were resuspended in 1XFA buffer (1% TritonX-100, 0.1% sodium deoxycholate, 0.1% SDS, 50 mM HEPES, 150 mM NaCl, 1 mM EDTA). Antibody S9.6 (25 μg) was pre-bound to 100 μL Protein A Dynabeads for 1 hour at 4°C in 1XFA buffer. 100 μg fragmented DNA was incubated with the S9.6-protein A beads for 2 hours at 4°C. Beads were washed in 5 successive washes: 1XFA, 1XFA with 0.5M NaCl, LiCl wash buffer (0.25M LiCl, 0.5% NP-40, 0.5% sodium deoxycholate, 1 mM EDTA, 10 mM Tris-HCl), twice with TE buffer. DNA was eluted in 300 μL elution buffer (1%SDS, 0.1M NaHCO3)for 2 hr at 65°C. Samples were then treated with 1 μL Proteinase K (20 mg/mL) for 1 hour at 42°C, extracted with phenol:chloroform, and then ethanol precipitated. The final DNA pellet was resuspended in 50 μL TE buffer. The percent hybrid signal for input and IP samples were quantified by qPCR. Sequencing libraries were prepared using the Qiagen GeneRead kit according to manufacturer's instructions. For spike-in normalized qPCR samples, *S. pombe* genomic DNA was prepared as described above and was added after RNase treatment in equal amounts.

Cell cycle synchronization—(alpha factor) Yeast strains were grown to an OD~0.2 and then synchronized by treatment with alpha factor (5 nM for *bar1Δ* or 5 μM for *BAR1*) for 2 hours. Visual inspection confirmed >90% of cells had shmoo-like morphology. Cells were then washed three times with YPD media lacking glucose supplemented with fresh 50 μg/mL pronase. Cells were released into indicated media and harvested as described below. (HU arrest) Yeast strains were grown to an OD~0.2 and then synchronized by treatment with 0.2 M HU for 3 hours. (Nocodazole arrest) Yeast strains were grown to an OD~0.2 and then synchronized by treatment with 15 μg/mL nocodazole for 3 hours.

Flow cytometry cell cycle analysis—Following alpha-factor arrest (see above), cells were released into fresh YPD supplemented with 50 μg/mL pronase. Yeast samples were harvested at the indicated time points and fixed in 1 mL 70% EtOH overnight at 4°C. Fixed cells were washed once in 50 mM Tris-HCl pH7.5, then treated with RNaseA overnight at 37°C. Following removal of RNaseA, cells were treated with Proteinase K and incubated at 37°C for 2 hours. Cells were resuspended in 50 mM Tris-HCl pH7.5. Cells

were briefly sonicated and then treated with 1 mL 50 mM Tris-HCl pH7.5 with 1μL of 1mM SYTOX green in DMSO. Flow cytometry analysis was immediately performed (Fortessa, BD Biosceince). Data was analyzed with FlowCytometryTools (https://eyurtsev.github.io/FlowCytometryTools/).

BrdU-IP—Following alpha-factor arrest (see above), cells were released into fresh YPD supplemented with 50 μg/mL pronase and 400 μg/mL BrdU. For HU-treated samples, hydroxyurea was added to a final concentration of 0.2 M HU. Cells were harvested after 30 minutes (untreated) or 60 minutes (HU treatment) by the addition of sodium azide to a final concentration of 0.1%. Cell pellets were washed once with cold 1XTBS and stored at −80°C. Cell pellets were resuspended in lysis buffer (2% SDS, 2% Triton-X100, 100 mM NaCl, 10 mM Tris pH 8.0, 1 mM EDTA) and 500 βL acid washed glass beads were added. Cells were lysed by vortexing for a total of 30 minutes at 4°C. Genomic DNA was isolated by phenol-chloroform isolation followed by ethanol precipitation with NaCl salt. DNA pellet was washed once with 70% ethanol and then resuspended in sterile water. DNA was treated with RNaseA/T1 for 30 minutes at 37°C followed by Proteinase K for 30 minutes at 50°C. Genomic DNA (gDNA) was column purified by a PCR purification kit. gDNA was fragmented by sonication to ~300 bp. Sonication efficiency was confirmed by gel electrophoresis. DNA concentration was measured by nanodrop and an equal amount of sonicated *S. pombe* genomic DNA was added to each sample. Input samples were removed immediately following spike-in addition. For next-generation sequencing experiments, libraries were prepared with the Qiagen GeneRead kit according to manufacturer's instructions prior to IP. For the IP, gDNA was boiled for 5 minutes at 95°C. Samples were incubated on ice for 3 minutes. 50 μL of gDNA (50-500 ng in EB) was combined with 50 μL anti-BrdU (1:250 in 2X IP buffer (2XPBS, 0.001% Triton-X100)) and incubated on a rotisserie for 2 hours at 4°C. 15 μL of washed Protein G Dynabeads was added. Samples were incubated on a rotisserie for 1 hour at 4°C. Samples were washed thrice in 1XIP buffer. Sample was eluted by the addition of TES and incubating for 10 min at 65°C. Samples were column purified prior to qPCR or sequence analysis.

Co-immunoprecipitation—For co-immunoprecipitation experiments, we used two epitope-tagging schemes. For Spt6 (Figures 3 and 4) and Spt6-YW (Figure 4), we used a C-terminal 3XFLAG epitope tag. For *spt6-50*, a nonsense mutation resulting in a C-terminal truncation of the protein, we used N-terminally tagged 3X-FLAG-Spt6 and 3X-FLAG-Spt6-50 (Figure 4). Yeast strains were harvested during mid-log phase (150 mL, OD~0.6). Cell pellets were washed once and stored at −80°C. Cell extracts were prepared by resuspending cell pellets in IP buffer (10% glycerol, 100 mM HEPES, 2mM EDTA, 150 mM KOAc, 0.1% NP-40, 10 mM MgOAc, 2 mM NaF, supplemented with 1 mM DTT and SIGMAFAST protease inhibitor tablet (Sigma) at time of use;[132]) and bead-beating for a total of 6 min at 4°C, with 5 minutes incubation on ice after every minute. For Benzonase treatment, 300U of Benzonase was added for 30 minutes rotating at 4°C. For all samples, cell lysate was then cleared for 20 minutes, 12500 rpm, 4°C. Total protein concentration was measured by Pierce BCA Protein Assay Kit (Thermo Fisher). For V5 immunoprecipitation, 5 μg anti-V5 (Invitrogen) was pre-bound to 30 μL Protein G Dynabeads for 1 hour at 4°C in 1XIP buffer. For FLAG immunoprecipitations, anti-FLAG-M2-FLAG affinity gel

(Sigma A2220) was washed and resuspended in 1XIP buffer. An equal concentration of total protein (10-20 μg/μL) was incubated with antibody-beads for 2 hours, rotating, 4°C. Samples were washed thrice in IP buffer and were eluted in 30 μL 3X protein loading dye (9% SDS, 10% BME, 187.5 mM Tris-HCl, 30% glycerol, bromophenol blue) at 105°C for 3 minutes. The beads were then spun down and the supernatant was transferred to a new tube and either stored or used for western blots (6% SDS-PAGE gels). The following antibodies were used for western blots analysis: 1:5,000 anti-FLAG-M2 (Sigma), 1:5,000 anti-V5 (Invitrogen), 1:2,500 anti-RNAPII-CTD (8WG16). Licor secondary antibodies were used. Images were quantified with ImageStudioLite. Quantifications were normalized to the signal for the wild-type tagged sample for each blot and the standard deviations were calculated in Microsoft Excel.

Chromatin immunoprecipitation (ChIP)—Following alpha-factor arrest (see above), samples were fixed with 1% formaldehyde at room temperature for 30 minutes. Crosslinking was quenched with the addition of glycine at a final concentration of 125 mM for 10 minutes. Samples were pelleted, washed with cold TBS, and flash frozen. Cell pellets were resuspended in LB140 (50 mM HEPES-KOH pH 7.5, 140 mM NaCl, 1 mM EDTA, 1% Triton-X, 0.1% sodium deoxycholate, 0.1% SDS, 100 μg leupeptin, 100 μg pepstatin A, 1/100 vol 100 mM PMSF, 1/250 vol. 0.1M DTT) and lysed by bead beating at 4°C for 8 minutes, with 5 minutes on ice in between every minute. The lysate was collected and the chromatin extract was pelleted and washed with LB140. The pellet was sonicated to ~200-400 bp fragments. Protein concentration was measured by Bradford and an equal amount (400 μg) was loaded per sample, with 5% w/w *S. pombe* chromatin spiked-in. Samples were diluted 1:1 with WB140 (50 mM HEPES-KOH pH 7.5, 140 mM NaCl, 1 mM EDTA, 1% Triton-X, 0.1% sodium deoxycholate), 5% input was removed, and incubated with 2.5 μg UM174 (MCM antisera) overnight at 4°C. 50 μL Protein G Dynabeads were added per sample and incubated at 4°C for 3 hours. Samples were washed twice with WB140, WB500 (50 mM HEPES-KOH pH 7.5, 500 mM NaCl, 1 mM EDTA, 1% Triton-X, 0.1% sodium deoxycholate), and WBLiCl (10 mM Tris-HCl pH 7.5, 250 mM LiCl, 1 mM EDTA, 0.5% NP-40, 0.5% sodium deoxycholate). Samples were washed once in TE. Samples were eluted with 100 μL TES at 65°C for 30 minutes. Crosslinking was reversed by incubating samples and inputs in TES at 65°C overnight. Inputs and IPs were treated with RNaseA/T1 and ProtK prior to column purification with Zymo DNA column kit according to manufactures instructions.

Rad52-foci microscopy—Cells were grown to mid-log phase. Samples were washed once with 1XPBS, briefly sonicated, and placed on a 2% agarose pad on imaging slide. Images were acquired with a Nikon Elipse Ti2 using 60X lens. Cells were manually staged based on cell morphology and foci were manually counted.

Bioinformatics analysis—A custom pipeline was used to process both BrdU-IP-seq, ChIP-seq, and DRIP-seq data. The custom pipeline was generated using the workflow manager Snakemake.[126] Briefly, data was aligned to a combined *S. cerevisiae* + *S. pombe* genome (*S. cerevisiae* R64-2-1, *S. pombe* ASM294v2) using Bowtie2.[127] Sequences were trimmed with cutadapt and processed using samtools,[128] bedtools, and deeptools[129] to

generate genome coverage tracks. This pipeline is available on the Winston lab GitHub (https://github.com/winston-lab). Deeptools was used to generate heatmaps of signal at desired regions and MACS2[133] was used to call peaks on individual samples. For HU-treated BrdU-IP samples and ChIP-seq data, irreproducible discovery rate (IDR) analysis was performed to identify common peaks across samples. As peaks were much broader and weaker for the BrdU-IP 30-minute samples, IDR analysis was not feasible. Instead, for 30-minute BrdU-IP samples, MACS2 peaks per sample were first filtered to isolate peaks larger than 1 kB in length and then merged to combine peaks within 5 kB. Peak regions present in both samples were then used as reproducible peaks across samples.

Northern blotting—RNA extraction from *S. cerevisiae* was done using hot acid phenol extraction. Ten μg of RNA was resuspended in RNA loading buffer (6% formaldehyde, 1X MOPS, 2.5% Ficoll, 10 mM Tris-HCl pH 7.5, 10 mM EDTA, 7 μg/ml ethidium bromide, 0.025% bromophenol blue, 0.025% Orange G), heated at 65°C for 10 minutes, then loaded on a 1% agarose/formaldehyde gel. The gel was run for 400 volt hours. Samples were denatured in the gel in 0.05M NaOH for 30 minutes at room temperature followed by neutralization in Tris-HCl, pH 7.5 for 30 minutes at room temperature. Samples were transferred to Genescreen membrane by upward capillary transfer in 1XSCC solution. The membrane was UV-crosslinked prior to hybridization. The membrane was incubated in pre-hybridization solution (50% deionized formamide, 10% dextran sulphate, 1M NaCl, 0.05M Tris-HCl pH 7.5, 0.1% SDS, 0.1% sodium pyrophosphate, 10X Denhardts reagent, 500 μg/mL denatured salmon sperm DNA) at 42°C for 5 hours. Membrane was hybridized to 32P-dATP labeled probe overnight at 42°C. The membrane was washed: 2 washes with 2XSCC for 15 minutes at room temperature, 2 washes with 2XSCC+0.5% SDS for 30 minutes at 65°C, and 2 washes with 0.1X SCC for 30 minutes at room temperature. Blots were imaged with a Typhoon phosphor-imager.

QUANTIFICATION AND STATISTICAL ANALYSIS

Statistical details, including the numbers of biological replicates (n) and the measures of precision (standard deviation), can be found in the figure legends and Method Details. In all cases, n represents the number of biological replicates. The values for n for the relevant experiments are provided in the legends of Figures 1,2, 3, 4, 5, 6, and 7. In all cases, error bars represent standard deviation, which was calculated using Microsoft Excel. Bioinformatics analysis was done as described in Method Details using a custom pipeline (https://doi.org/10.5281/zenodo.7644131) and tools that are listed in the key resources table.

Supplementary Material

Refer to Web version on PubMed Central for supplementary material.

ACKNOWLEDGMENTS

We thank Kaia Mattioli and James Warner for helpful comments on the manuscript. We also thank Stephen Bell and Luis Martinez for supplying anti-MCM antisera and advice on MCM ChIP-seq; Lorenzo Costantino and Doug Koshl and for advice on DRIP and for supplying S9.6 antisera; Etienne Schwob for supplying plasmids and advice for the BrdU experiments; David Waterman and Jim Haber for advice on using Rad52-YFP, and Nick Rhind for supplying *S. pombe* strains for BrdU experiments. We are also grateful to Marco Fumasoni and Andrew Murray for guidance on the flow cytometry experiments and Jessica King for help with experiments. Part of this research

was conducted on the O2 High Performance Computer Cluster supported by the Research Computing Group at Harvard Medical School. This work was supported by grants from the NSF and from the Landry Cancer Biology Consortium to C.L.W.M. and NIH grant R01GM135251 to F.W.

REFERENCES

1. Warren C, and Shechter D (2017). Fly Fishing for Histones: Catch and Release by Histone Chaperone Intrinsically Disordered Regions and Acidic Stretches. J. Mol. Biol 429, 2401–2426. 10.1016/j.jmb.2017.06.005. [PubMed: 28610839]
2. Hammond CM, Strømme CB, Huang H, Patel DJ, and Groth A (2017). Histone chaperone networks shaping chromatin function. Nat. Rev. Mol. Cell Biol 18, 141–158. 10.1038/nrm.2016.159. [PubMed: 28053344]
3. Nacev BA, Feng L, Bagert JD, Lemiesz AE, Gao J, Soshnev AA, Kundra R, Schultz N, Muir TW, and Allis CD (2019). The expanding landscape of 'oncohistone' mutations in human cancers. Nature 567, 473–478. 10.1038/s41586-019-1038-1. [PubMed: 30894748]
4. Plass C, Pfister SM, Lindroth AM, Bogatyrova O, Claus R, and Lichter P (2013). Mutations in regulators of the epigenome and their connections to global chromatin patterns in cancer. Nat. Rev. Genet 14, 765–780. 10.1038/nrg3554. [PubMed: 24105274]
5. Ray-Gallet D, and Almouzni G (2022). H3–H4 histone chaperones and cancer. Curr. Opin. Genet. Dev 73, 101900. 10.1016/j.gde.2022.101900. [PubMed: 35183848]
6. Clark-Adams CD, and Winston F (1987). The SPT6 gene is essential for growth and is required for delta-mediated transcription in Saccharomyces cerevisiae. Mol. Cell Biol 7, 679–686. [PubMed: 3029564]
7. Neigeborn L, Celenza JL, and Carlson M (1987). SSN20 is an essential gene with mutant alleles that suppress defects in SUC2 transcription in Saccharomyces cerevisiae. Mol. Cell Biol 7, 672–678. 10.1128/mcb.7.2.672-678.1987. [PubMed: 3547080]
8. Nishiwaki K, Sano T, and Miwa J (1993). emb-5, a gene required for the correct timing of gut precursor cell division during gastrulation in Caenorhabditis elegans, encodes a protein similar to the yeast nuclear protein SPT6. Mol. Gen. Genet 239, 313–322. 10.1007/BF00276929. [PubMed: 8391108]
9. Keegan BR, Feldman JL, Lee DH, Koos DS, Ho RK, Stainier DYR, and Yelon D (2002). The elongation factors Pandora/Spt6 and Foggy/Spt5 promotetranscription in the zebrafish embryo. Development (Camb.) 129, 1623–1632.
10. Kok FO, Oster E, Mentzer L, Hsieh JC, Henry CA, and Sirotkin HI (2007). The role ofthe SPT6 chromatin remodeling factor in zebrafish embryogenesis. Dev. Biol 307, 214–226. 10.1016/j.yd-bio.2007.04.039. [PubMed: 17570355]
11. Bourbon HM, Gonzy-Treboul G, Peronnet F, Alin MF, Ardourel C, Benassayag C, Cribbs D, Deutsch J, Ferrer P, Haenlin M, et al. (2002). A P-insertion screen identifying novel X-linked essential genes in Drosophila. Mech. Dev 110, 71–83. [PubMed: 11744370]
12. Ardehali MB, Yao J, Adelman K, Fuda NJ, Petesch SJ, Webb WW, and Lis JT (2009). Spt6 enhancesthe elongation rate of RNA polymerase II in vivo. EMBO J. 28,1067–1077. 10.1038/emboj.2009.56. [PubMed: 19279664]
13. Wang AH, Juan AH, Ko KD, Tsai PF, Zare H, Dell'Orso S, and Sartorelli V (2017). The Elongation Factor Spt6 Maintains ESC Pluripotency by Controlling Super-Enhancers and Counteracting Polycomb Proteins. Mol. Cell 68, 398–413.e6. 10.1016/j.molcel.2017.09.016. [PubMed: 29033324]
14. Vo DT, Fuller MR, Tindle C, Anandachar MS, Das S, Sahoo D, and Ghosh P (2021). SPT6 loss permits the transdifferentiation of keratinocytes into an intestinal fate that resembles Barrett's metaplasia. iScience 24, 103121. 10.1016/j.isci.2021.103121. [PubMed: 34622168]
15. Wang AH, Zare H, Mousavi K, Wang C, Moravec CE, Sirotkin HI, Ge K, Gutierrez-Cruz G, and Sartorelli V (2013). The histone chaperone Spt6 coordinates histone H3K27 demethylation and myogenesis. EMBO J. 32, 1075–1086. 10.1038/emboj.2013.54. [PubMed: 23503590]
16. Okazaki IM, Okawa K, Kobayashi M, Yoshikawa K, Kawamoto S, Nagaoka H, Shinkura R, Kitawaki Y, Taniguchi H, Natsume T, et al. (2011). Histone chaperone Spt6 is required for class

switch recombination but not somatic hypermutation. Proc. Natl. Acad. Sci. USA 108, 7920–7925. 10.1073/pnas.1104423108. [PubMed: 21518874]

17. Begum NA, Stanlie A, Nakata M, Akiyama H, and Honjo T (2012). The histone chaperone Spt6 is required for activation-induced cytidine deaminase target determination through H3K4me3 regulation. J. Biol. Chem 287, 32415–32429. 10.1074/jbc.M112.351569. [PubMed: 22843687]
18. Karczewski KJ, Francioli LC, Tiao G, Cummings BB, Alföldi J, Wang Q, Collins RL, Laricchia KM, Ganna A, Birnbaum DP, et al. (2020). The mutational constraint spectrum quantified from variation in 141,456 humans. Nature 581, 434–443. 10.1038/s41586-020-2308-7. [PubMed: 32461654]
19. Vos SM, Farnung L, Urlaub H, Cramer P, Linden A, Urlaub H, and Cramer P (2018). Structure of activated transcription complex Pol II–DSIF–PAF–SPT6. Nature 560, 601–606. 10.1038/s41586-018-0442-2. [PubMed: 30135580]
20. Ehara H, Kujirai T, Shirouzu M, Kurumizaka H, and Sekine SI (2022). Structural basis of nucleosome disassembly and reassembly by RNAPII elongation complex with FACT. Science 377. 10.1126/science.abp9466.
21. Filipovski M, Soffers JHM, Vos SM, and Farnung L (2022). Structural basis of nucleosome retention during transcription elongation. Science 376, 1313–1316. 10.1126/science.abo3851. [PubMed: 35709268]
22. Vos SM, Farnung L, Linden A, Urlaub H, and Cramer P (2020). Structure of complete Pol II–DSIF–PAF–SPT6 transcription complex reveals RTF1 allosteric activation. Nat. Struct. Mol. Biol 27, 668–677. 10.1038/s41594-020-0437-1. [PubMed: 32541898]
23. Yoh SM, Cho H, Pickle L, Evans RM, and Jones KA (2007). The Spt6 SH2 domain binds Ser2-P RNAPII to direct Iws1-dependent mRNA splicing and export. Genes Dev. 21, 160–174. 10.1101/gad.1503107. [PubMed: 17234882]
24. Diebold ML, Loeliger E, Koch M, Winston F, Cavarelli J, and Romier C (2010). Noncanonical tandem SH2 enables interaction of elongation factor Spt6 with RNA polymerase II. J. Biol. Chem 285, 38389–38398. 10.1074/jbc.M110.146696. [PubMed: 20926373]
25. Sun M, Larivire L, Dengl S, Mayer A, and Cramer P (2010). A tandem SH2 domain in transcription elongation factor Spt6 binds the phosphorylated RNA polymerase II C-terminal repeat domain (CTD). J. Biol. Chem 285, 41597–41603. 10.1074/jbc.M110.144568. [PubMed: 20926372]
26. Close D, Johnson SJ, Sdano MA, McDonald SM, Robinson H, Formosa T, and Hill CP (2011). Crystal structures of the S. cerevisiae Spt6 core and C-terminal tandem SH2 domain. J. Mol. Biol 408, 697–713. 10.1016/j.jmb.2011.03.002. [PubMed: 21419780]
27. Sdano MA, Fulcher JM, Palani S, Chandrasekharan MB, Parnell TJ, Whitby FG, Formosa T, and Hill CP (2017). A novel SH2 recognition mechanism recruits Spt6 to the doubly phosphorylated RNA polymerase II linker at sites of transcription. Elife 6, e28723–24. 10.7554/eLife.28723. [PubMed: 28826505]
28. Bortvin A, and Winston F (1996). Evidence that Spt6p controls chromatin structure by a direct interaction with histones. Science 272, 1473–1476. 10.1126/science.272.5267.1473. [PubMed: 8633238]
29. McDonald SM, Close D, Xin H, Formosa T, and Hill CP (2010). Structure and Biological Importance of the Spn1-Spt6 Interaction, and Its Regulatory Role in Nucleosome Binding. Mol. Cell 40, 725–735. 10.1016/j.molcel.2010.11.014. [PubMed: 21094070]
30. McCullough L, Connell Z, Petersen C, and Formosa T (2015). The abundant histone chaperones Spt6 and FACT collaborate to assemble, inspect, and maintain chromatin structure in saccharomyces cerevisiae. Genetics 201, 1031–1045. 10.1534/genetics.115.180794. [PubMed: 26416482]
31. Kasiliauskaite A, Kubicek K, Klumpler T, Zanova M, Zapletal D, Koutna E, Novacek J, and Stefl R (2022). Cooperation between intrinsically disordered and ordered regions of Spt6 regulates nucleosome and Pol II CTD binding, and nucleosome assembly. Nucleic Acids Res. 50, 5961–5973. 10.1093/nar/gkac451. [PubMed: 35640611]

32. Li S, Edwards G, Radebaugh CA, Luger K, and Stargell LA (2022). Spn1 and Its Dynamic Interactions with Spt6, Histones and Nucleosomes. J. Mol. Biol 434, 167630. 10.1016/j.jmb.2022.167630. [PubMed: 35595162]
33. Adkins MW, and Tyler JK (2006). Transcriptional activators are dispensable fortranscription in the absence of Spt6-mediated chromatin reassembly of promoter regions. Mol. Cell 21, 405–416. 10.1016/j.molcel.2005.12.010. [PubMed: 16455495]
34. Ivanovska I, Jacques PE, Rando OJ, Robert F, and Winston F (2011). Control of Chromatin Structure by Spt6: Different Consequences in Coding and Regulatory Regions. Mol. Cell Biol 31, 531–541. 10.1128/MCB.01068-10. [PubMed: 21098123]
35. Endoh M, Zhu W, Hasegawa J, Watanabe H, Kim D-K, Aida M, Inukai N, Narita T, Yamada T, Furuya A, et al. (2004). Human Spt6 stimulates transcription elongation by RNA polymerase II in vitro. Mol. Cell Biol 24, 3324–3336. 10.1128/MCB.24.8.3324. [PubMed: 15060154]
36. Narain A, Bhandare P, Adhikari B, Backes S, Eilers M, Dölken L, Schlosser A, Erhard F, Baluapuri A, and Wolf E (2021). Targeted protein degradation reveals a direct role of SPT6 in RNAPII elongation and termination. Mol. Cell 81, 3110–3127.e14. 10.1016/j.molcel.2021.06.016. [PubMed: 34233157]
37. Žumer K, Maier KC, Farnung L, Jaeger MG, Rus P, Winter G, and Cramer P (2021). Two distinct mechanisms of RNA polymerase II elongation stimulation in vivo. Mol. Cell 81, 3096–3109.e8. 10.1016/j.molcel.2021.05.028. [PubMed: 34146481]
38. Kaplan CD, Laprade L, and Winston F (2003). Transcription elongation factors repress transcription initiation from cryptic sites. Science 301, 1096–1099. 10.1126/science.1087374. [PubMed: 12934008]
39. Doris SM, Chuang J, Viktorovskaya O, Murawska M, Spatt D, Churchman LS, and Winston F (2018). Spt6 Is Required for the Fidelity of Promoter Selection. Mol. Cell 72,687–699.e6. 10.1016/j.molcel.2018.09.005. [PubMed: 30318445]
40. Cheung V, Chua G, Batada NN, Landry CR, Michnick SW, Hughes TR, and Winston F (2008). Chromatin- and transcription-related factors repress transcription from within coding regions throughout the Saccharomyces cerevisiae genome. PLoS Biol. 6, e277–e2562. 10.1371/journal.pbio.0060277. [PubMed: 18998772]
41. Uwimana N, Collin P, Jeronimo C, Haibe-Kains B, and Robert F (2017). Bidirectional terminators in Saccharomyces cerevisiae prevent cryptic transcription from invading neighboring genes. Nucleic Acids Res. 45, 6417–6426. 10.1093/nar/gkx242. [PubMed: 28383698]
42. Gouot E, Bhat W, Rufiange A, Fournier E, Paquet E, and Nourani A (2018). Casein kinase 2 mediated phosphorylation of Spt6 modulates histone dynamics and regulates spurious transcription. Nucleic Acids Res. 46, 7612–7630. 10.1093/nar/gky515. [PubMed: 29905868]
43. Nojima T, Tellier M, Foxwell J, Ribeiro de Almeida C, Tan-Wong SM, Dhir S, Dujardin G, Dhir A, Murphy S, and Proudfoot NJ (2018). Deregulated Expression of Mammalian lncRNA through Loss of SPT6 Induces R-Loop Formation, Replication Stress, and Cellular Senescence. Mol. Cell 72, 970–984.e7. 10.1016/j.mol-cel.2018.10.011. [PubMed: 30449723]
44. Kaplan CD, Holland MJ, and Winston F (2005). Interaction between transcription elongation factors and mRNA 3′-end formation at the Saccharomyces cerevisiae GAL10-GAL7 locus. J. Biol. Chem 280, 913–922. 10.1074/jbc.M411108200. [PubMed: 15531585]
45. van Bakel H, Tsui K, Gebbia M, Mnaimneh S, Hughes TR, and Nislow C (2013). A Compendium of Nucleosome and Transcript Profiles Reveals Determinants of Chromatin Architecture and Transcription. PLoS Genet. 9, e1003479. 10.1371/journal.pgen.1003479. [PubMed: 23658529]
46. DeGennaro CM, Alver BH, Marguerat S, Stepanova E, Davis CP, Bähler J, Park PJ, and Winston F (2013). Spt6 Regulates Intragenic and Antisense Transcription, Nucleosome Positioning, and Histone Modifications Genome-Wide in Fission Yeast. Mol. Cell Biol 33, 4779–4792. 10.1128/mcb.01068-13. [PubMed: 24100010]
47. Perales R, Erickson B, Zhang L, Kim H, Valiquett E, and Bentley D (2013). Gene promoters dictate histone occupancy within genes. EMBO J. 32, 2645–2656. 10.1038/emboj.2013.194. [PubMed: 24013117]

48. Jeronimo C, Poitras C, and Robert F (2019). Histone Recycling by FACT and Spt6 during Transcription Prevents the Scrambling of Histone Modifications. Cell Rep. 28,1206–1218.e8. 10.1016/j.cel-rep.2019.06.097. [PubMed: 31365865]

49. Petruk S, Sedkov Y, Riley KM, Hodgson J, Schweisguth F, Hirose S, Jaynes JB, Brock HW, and Mazo A (2006). Transcription of bxd Noncoding RNAs Promoted by Trithorax Represses Ubx in cis by Transcriptional Interference. Cell 127, 1209–1221. 10.1016/j.cell.2006.10.039. [PubMed: 17174895]

50. Kato H, Okazaki K, Iida T, Nakayama JI, Murakami Y, and Urano T (2013). Spt6 preventstranscription-coupled loss of posttranslationally modified histone H3. Sci. Rep 3, 2186. 10.1038/srep02186. [PubMed: 23851719]

51. Chen S, Ma J, Wu F, Xiong LJ, Ma H, Xu W, Lv R, Li X, Villen J, Gygi SP, et al. (2012). The histone H3 Lys 27 demethylase JMJD3 regulates gene expression by impacting transcriptional elongation. Genes Dev. 26, 1364–1375. 10.1101/gad.186056.111. [PubMed: 22713873]

52. Yoh SM, Lucas JS, and Jones KA (2008). The Iws1:Spt6:CTD complex controls cotranscriptional mRNA biosynthesis and HYPB/Setd2-mediated histone H3K36 methylation. Genes Dev. 22, 3422–3434. 10.1101/gad.1720008. [PubMed: 19141475]

53. Youdell ML, Kizer KO, Kisseleva-Romanova E, Fuchs SM, Duro E, Strahl BD, and Mellor J (2008). Roles for Ctk1 and Spt6 in Regulating the Different Methylation States of Histone H3 Lysine 36. Mol. Cell Biol 28, 4915–4926. 10.1128/MCB.00001-08. [PubMed: 18541663]

54. Gopalakrishnan R, Marr SK, Kingston RE, and Winston F (2019). A conserved genetic interaction between Spt6 and Set2 regulates H3K36 methylation. Nucleic Acids Res. 47, 3888–3903. 10.1093/nar/gkz119. [PubMed: 30793188]

55. Carrozza MJ, Li B, Florens L, Suganuma T, Swanson SK, Lee KK, Shia WJ, Anderson S, Yates J, Washburn MP, and Workman JL (2005). Histone H3 methylation by Set2 directs deacetylation of coding regions by Rpd3S to suppress spurious intragenic transcription. Cell 123, 581–592. 10.1016/j.cell.2005.10.023. [PubMed: 16286007]

56. Malagón F, and Aguilera A (1996). Differential intrachromosomal hyper-recombination phenotype of spt4 and spt6 mutants of S. cerevisiae. Curr. Genet 30, 101–106. 10.1007/s002940050107. [PubMed: 8660457]

57. Malagón F, and Aguilera A (2001). Yeast spt6-140 mutation, affecting chromatin and transcription, preferentially increases recombination in which Rad51p-mediated strand exchange is dispensable. Genetics 158, 597–611. 10.1093/genetics/158.2.597. [PubMed: 11404325]

58. Basrai MA, Kingsbury J, Koshland D, Spencer F, and Hieter P (1996). Faithful chromosome transmission requires Spt4p, a putative regulator of chromatin structure in Saccharomyces cerevisiae. Mol. Cell Biol 16, 2838–2847. 10.1128/MCB.16.6.2838. [PubMed: 8649393]

59. Diebold ML, Koch M, Loeliger E, Cura V, Winston F, Cavarelli J, and Romier C (2010). The structure of an Iws1/Spt6 complex reveals an interaction domain conserved in TFIIS, Elongin A and Med26. EMBO J. 29, 3979–3991. 10.1038/emboj.2010.272. [PubMed: 21057455]

60. Viktorovskaya O, Chuang J, Jain D, Reim NI, López-Rivera F, Murawska M, Spatt D, Churchman LS, Park PJ, and Winston F (2021). Essential histone chaperones collaborate to regulate transcription and chromatin integrity. Genes Dev. 35, 698–712. 10.1101/GAD.348431.121. [PubMed: 33888559]

61. Nishimura K, Fukagawa T, Takisawa H, Kakimoto T, and Kanemaki M (2009). An auxin-based degron system for the rapid depletion of proteins in nonplant cells. Nat. Methods 6, 917–922. 10.1038/nmeth.1401. [PubMed: 19915560]

62. Lengronne A, Pasero P, Bensimon A, and Schwob E (2001). Monitoring S phase progression globally and locally using BrdU incorporation in TK+ yeast strains. Nucleic Acids Res. 29, 1433–1442. 10.1093/nar/29.7.1433. [PubMed: 11266543]

63. Sivakumar S, Porter-Goff M, Patel PK, Benoit K, and Rhind N (2004). In vivo labeling of fission yeast DNA with thymidine and thymidine analogs. Methods 33, 213–219. 10.1016/j.ymeth.2003.11.016. [PubMed: 15157888]

64. Winston F, Chaleff DT, Valent B, and Fink GR (1984). Mutations affecting Ty-mediated expression of the HIS4 gene of Saccharomyces cerevisiae. Genetics 107, 179–197. [PubMed: 6329902]

65. Dronamraju R, and Strahl BD (2014). A feed forward circuit comprising Spt6, Ctk1 and PAF regulates Pol II CTD phosphorylation and transcription elongation. Nucleic Acids Res. 42, 870–881. 10.1093/nar/gkt1003. [PubMed: 24163256]
66. Chu Y, Sutton A, Sternglanz R, and Prelich G (2006). The Bur1 Cyclin-Dependent Protein Kinase Is Required for the Normal Pattern of Histone Methylation by Set2. Mol. Cell Biol 26, 3029–3038. 10.1128/MCB.26.8.3029-3038.2006. [PubMed: 16581778]
67. Zeman MK, and Cimprich KA (2014). Causes and consequences of replication stress. Nat. Cell Biol 16, 2–9. 10.1038/ncb2897. [PubMed: 24366029]
68. Mathiasen DP, and Lisby M (2014). Cell cycle regulation of homologous recombination in Saccharomyces cerevisiae. FEMS Microbiol. Rev 38, 172–184. 10.1111/1574-6976.12066. [PubMed: 24483249]
69. Lisby M, Rothstein R, and Mortensen UH (2001). Rad52 forms DNA repair and recombination centers during S phase. Proc. Natl. Acad. Sci. USA 98, 8276–8282. 10.1073/pnas.121006298. [PubMed: 11459964]
70. Connell Z, Parnell TJ, Mccullough LL, Hill CP, and Formosa T (2022). The interaction between the Spt6-tSH2 domain and Rpb1 affects multiple functions of RNA Polymerase II. Nucleic Acids Res. 50,784–802. 10.1093/nar/gkab1262. [PubMed: 34967414]
71. Simon AC, Zhou JC, Perera RL, Van Deursen F, Evrin C, Ivanova ME, Kilkenny ML, Renault L, Kjaer S, Matak-Vinkovi D, et al. (2014). A Ctf4 trimer couples the CMG helicase to DNA polymerase ί± in the eukaryotic replisome. Nature 510, 293–297. 10.1038/nature13234. [PubMed: 24805245]
72. Gambus A, Van Deursen F, Polychronopoulos D, Foltman M, Jones RC, Edmondson RD, Calzada A, and Labib K (2009). A key role for Ctf4 in coupling the MCM2-7 helicase to DNA polymerase α within the eukaryotic replisome. EMBO J. 28, 2992–3004. 10.1038/emboj.2009.226. [PubMed: 19661920]
73. Villa F, Simon AC, Ortiz Bazan MA, Kilkenny ML, Wirthensohn D, Wightman M, Matak-Vinkovíc D, Pellegrini L, and Labib K (2016). Ctf4 Is a Hub in the Eukaryotic Replisome that Links Multiple CIP-Box Proteins to the CMG Helicase. Mol. Cell 63, 385–396. 10.1016/j.molcel.2016.06.009. [PubMed: 27397685]
74. Tanaka H, Katou Y, Yagura M, Saitoh K, Itoh T, Araki H, Bando M, and Shirahige K (2009). Ctf4 coordinates the progression of helicase and DNA polymerase α. Gene Cell. 14, 807–820. 10.1111/j.1365-2443.2009.01310.x.
75. Pardo B, Crabbé L, and Pasero P (2016). Signaling pathways of replication stress in yeast. FEMS Yeast Res. 17, fow101–11. 10.1093/femsyr/fow101.
76. Musacchio A (2015). The Molecular Biology of Spindle Assembly Checkpoint Signaling Dynamics. Curr. Biol 25, R1002–R1018. 10.1016/j.cub.2015.08.051. [PubMed: 26485365]
77. Raghuraman MK, Winzeler EA, Collingwood D, Hunt S, Wodicka L, Conway A, Lockhart DJ, Davis RW, Brewer BJ, Fangman WL, et al. (2001). Replication Dynamics of the Yeast. Science 294, 115–121. 10.1126/science.294.5540.115. [PubMed: 11588253]
78. Feng W, Collingwood D, Boeck ME, Fox LA, Alvino GM, Fangman WL, Raghuraman MK, and Brewer BJ (2006). Challenged Yeasts Identifies Origins of Replication. Nat. Cell Biol 8, 148–155. 10.1038/ncb1358.Genomic. [PubMed: 16429127]
79. Nieduszynski CA, Knox Y, and Donaldson AD (2006). Genome-wide identification of replication origins in yeast by comparative genomics. Genes Dev. 20, 1874–1879. 10.1101/gad.385306. [PubMed: 16847347]
80. Hawkins M, Retkute R, Müller CA, Saner N, Tanaka TU, deMoura APS, and Nieduszynski CA (2013). High-Resolution Replication Profiles Define the Stochastic Nature of Genome Replication Initiation and Termination. Cell Rep. 5, 1132–1141. 10.1016/j.celrep.2013.10.014. [PubMed: 24210825]
81. Poli J, Gerhold CB, Tosi A, Hustedt N, Seeber A, Sack R, Herzog F , Pasero P, Shimada K, Hopfner KP, and Gasser SM (2016). Mec1, INO80, and the PAF1 complex cooperate to limit transcription replication conflicts through RNAPII removal during replication stress. Genes Dev. 30, 337–354. 10.1101/gad.273813.115. [PubMed: 26798134]

82. Bell SP, and Labib K (2016). Chromosome duplication in Saccharomyces cerevisiae. Genetics 203,1027–1067. 10.1534/genetics.115.186452. [PubMed: 27384026]

83. Labib K, Diffley JF, and Kearsey SE (1999). G1-phase and B-type cyclins exclude the DNA-replication factor Mcm4 from the nucleus. Nat. Cell Biol 1, 415–422. 10.1038/15649. [PubMed: 10559985]

84. Yamamoto K, Makino N, Nagai M, Araki H, and Ushimaru T (2018). CDK phosphorylation regulates Mcm3 degradation in budding yeast. Biochem. Biophys. Res. Commun 506, 680–684. 10.1016/j.bbrc.2018.10.149. [PubMed: 30376991]

85. Nguyen VQ, Co C, Irie K, and Li JJ (2000). Clb/Cdc28 kinases promote nuclear export of the replication initiator proteins Mcm2–7. Curr. Biol 10, 195–205. 10.1016/s0960-9822(00)00337-7. [PubMed: 10704410]

86. Swanson MS, Carlson M, and Winston F (1990). SPT6, an essential gene that affects transcription in Saccharomyces cerevisiae, encodes a nuclear protein with an extremely acidic amino terminus. Mol. Cell Biol 10, 4935–4941. 10.1128/mcb.10.9.4935-4941.1990. [PubMed: 2201908]

87. Dronamraju R, Hepperla AJ, Shibata Y, Adams AT, Magnuson T, Davis IJ, and Strahl BD (2018). Spt6 Association with RNA Polymerase II Directs mRNA Turnover During Transcription. Mol. Cell 70, 1054–1066.e4. 10.1016/j.molcel.2018.05.020. [PubMed: 29932900]

88. Obara EAA, Aguilar-Morante D, Rasmussen RD, Frias A, Vitting-Serup K, Lim YC, Elbæk KJ, Pedersen H, Vardouli L, Jensen KE, et al. (2020). SPT6-driven error-free DNA repair safeguards genomic stability of glioblastoma cancer stem-like cells. Nat. Commun 11, 4709. 10.1038/s41467-020-18549-8. [PubMed: 32948765]

89. Aguilera A, and García-Muse T (2013). Causes of genome instability. Annu. Rev. Genet 47, 1–32. 10.1146/annurev-genet-111212-133232. [PubMed: 23909437]

90. Herrera-Moyano E, Mergui X, García-Rubio ML, Barroso S, and Aguilera A (2014). The yeast and human FACT chromatin-reorganizing complexes solve R-loop-mediated transcription–replication conflicts. Genes Dev. 28, 735–748. 10.1101/gad.234070.113. [PubMed: 24636987]

91. Bayona-Feliu A, and Aguilera A (2021). The role of chromatin at transcription-replication conflicts as a genome safeguard. Biochem. Soc. Trans 49, 2727–2736. 10.1042/BST20210691. [PubMed: 34821364]

92. Crossley MP, Bocek M, and Cimprich KA (2019). R-Loops as Cellular Regulators and Genomic Threats. Mol. Cell 73, 398–411. 10.1016/j.molcel.2019.01.024. [PubMed: 30735654]

93. Castillo-Guzman D, and Chédin F (2021). Defining R-loop classes and their contributions to genome instability. DNA Repair 106, 103182. 10.1016/j.dnarep.2021.103182. [PubMed: 34303066]

94. Kemiha S, Poli J, Lin YL, Lengronne A, and Pasero P (2021). Toxic R-loops: Cause or consequence of replication stress? DNA Repair 107, 103199. 10.1016/j.dnarep.2021.103199. [PubMed: 34399314]

95. Wahba L, Costantino L, Tan FJ, Zimmer A, and Koshland D (2016). S1-DRIP-seq identifies high expression and polyA tracts as major contributors to R-loop formation. Genes Dev. 30, 1327–1338. 10.1101/gad.280834.116. [PubMed: 27298336]

96. Belsky JA, Macalpine HK, Lubelsky Y, Hartemink AJ, and Macalpine DM (2015). Genome-wide chromatin foot printing reveals changes in replication origin architecture induced by pre-RC assembly. Genes Dev. 29, 212–224. 10.1101/gad.247924.114. [PubMed: 25593310]

97. Dukaj L, and Rhind N (2021). The capacity of origins to load mcm establishes replication timing patterns. PLoS Genet. 17, e1009467–28. 10.1371/journal.pgen.1009467. [PubMed: 33764973]

98. Foss EJ, Sripathy S, Gatbonton-Schwager T, Kwak H, Thiesen AH, Lao U, and Bedalov A (2021). Chromosomal Mcm2-7 distribution and the genome replication program in species from yeast to humans. PLoS Genet. 17, e1009714. 10.1371/journal.pgen.1009714. [PubMed: 34473702]

99. Das SP, Borrman T, Liu VWT, Yang SCH, Bechhoefer J, and Rhind N (2015). Replication timing is regulated by the number of MCMs loaded at origins. Genome Res. 25, 1886–1892. 10.1101/gr.195305.115. [PubMed: 26359232]

100. Mousson F, Ochsenbein F, and Mann C (2007). The histone chaperone Asf1 at the crossroads of chromatin and DNA checkpoint pathways. Chromosoma 116, 79–93. 10.1007/s00412-006-0087-z. [PubMed: 17180700]

101. Formosa T, and Winston F (2020). The role of FACT in managing chromatin: Disruption, assembly, or repair? Nucleic Acids Res. 48, 11929–11941. 10.1093/nar/gkaa912. [PubMed: 33104782]
102. Li S, Wasserman MR, Yurieva O, Bai L, O'Donnell ME, and Liu S (2022). Origin recognition complex harbors an intrinsic nucleosome remodeling activity. Proc. Natl. Acad. Sci. USA 119, e2211568119. 10.1073/pnas.2211568119. [PubMed: 36215487]
103. Azmi IF, Watanabe S, Maloney MF, Kang S, Belsky JA, MacAlpine DM, Peterson CL, and Bell SP (2017). Nucleosomes influence multiple steps during replication initiation. Elife 6, e22512–23. 10.7554/eLife.22512. [PubMed: 28322723]
104. Eaton ML, Galani K, Kang S, Bell SP, and MacAlpine DM (2010). Conserved nucleosome positioning defines replication origins. Genes Dev. 24, 748–753. 10.1101/gad.1913210. [PubMed: 20351051]
105. Berbenetz NM, Nislow C, and Brown GW (2010). Diversity of Eukaryotic DNA replication origins revealed by Genome-wide analysis of chromatin structure. PLoS Genet. 6, e1001092. 10.1371/journal.pgen.1001092. [PubMed: 20824081]
106. Breier AM, Chatterji S, and Cozzarelli NR (2004). Prediction of Saccharomyces cerevisiae replication origins. Genome Biol. 5, R22. 10.1186/gb-2004-5-4-r22. [PubMed: 15059255]
107. Lipford JR, and Bell SP (2001). Nucleosomes Positioned by ORC Facilitate the Initiation of DNA Replication. Mol. Cell 7, 21–30. 10.1016/s1097-2765(01)00151-4. [PubMed: 11172708]
108. Unnikrishnan A, Gafken PR, and Tsukiyama T (2010). Dynamic changes in histone acetylation regulate origins of DNA replication. Nat. Struct. Mol. Biol. 17, 430–437. 10.1038/nsmb.1780. [PubMed: 20228802]
109. Pryde F, Jain D, Kerr A, Curley R, Mariotti FR, and Vogelauer M (2009). H3 K36 methylation helps determine the timing of Cdc45 association with replication origins. PLoS One 4, e5882. 10.1371/journal.pone.0005882. [PubMed: 19521516]
110. Vogelauer M, Rubbi L, Lucas I, Brewer BJ, and Grunstein M (2002). Time of Replication Origin Firing. Mol. Cell 10, 1223–1233. [PubMed: 12453428]
111. Soudet J, Gill JK, and Stutz F (2018). Noncoding transcription influences the replication initiation program through chromatin regulation. Genome Res. 28, 1882–1893. 10.1101/gr.239582.118. [PubMed: 30401734]
112. Candelli T, Gros J, and Libri D (2018). Pervasive transcription fine-tunes replication origin activity. Elife 7, e40802–37. 10.7554/eLife.40802. [PubMed: 30556807]
113. Liu Y, Ai C, Gan T, Wu J, Jiang Y, Liu X, Lu R, Gao N, Li Q, Ji X, and Hu J (2021). Transcription shapes DNA replication initiation to preserve genome integrity. Genome Biol. 22, 176–27. 10.1186/s13059-021-02390-3. [PubMed: 34108027]
114. Lee CSK, Cheung MF, Li J, Zhao Y, Lam WH, Ho V, Rohs R, Zhai Y, Leung D, and Tye BK (2021). Humanizing the yeast origin recognition complex. Nat. Commun 12, 33–11. 10.1038/s41467-020-20277-y. [PubMed: 33397927]
115. Cristini A, Groh M, Kristiansen MS, and Gromak N (2018). RNA/DNA Hybrid Interactome Identifies DXH9 as a Molecular Player in Transcriptional Termination and R-Loop-Associated DNA Damage. Cell Rep. 23, 1891–1905. 10.1016/j.celrep.2018.04.025. [PubMed: 29742442]
116. Sanz LA, Hartono SR, Lim YW, Steyaert S, Rajpurkar A, Ginno PA, Xu X, and Chédin F (2016). Prevalent, Dynamic, and Conserved R-Loop Structures Associate with Specific Epigenomic Signatures in Mammals. Mol. Cell 63, 167–178. 10.1016/j.molcel.2016.05.032. [PubMed: 27373332]
117. Zardoni L, Nardini E, Brambati A, Lucca C, Choudhary R, Loperfido F, Sabbioneda S, and Liberi G (2021). Elongating RNA polymerase II and RNA:DNA hybrids hinder fork progression and gene expression at sites of head-on replication-transcription collisions. Nucleic Acids Res. 49, 12769–12784. 10.1093/nar/gkab1146. [PubMed: 34878142]
118. Nourani A, Robert F, and Winston F (2006). Evidence that Spt2/Sin1, an HMG-Like Factor, Plays Roles in Transcription Elongation, Chromatin Structure, and Genome Stability in Saccharomyces cerevisiae. Mol. Cell Biol 26, 1496–1509. 10.1128/MCB.26.4.1496-1509.2006. [PubMed: 16449659]

119. Jeronimo C, Watanabe S, Kaplan CD, Peterson CL, and Robert F (2015). The Histone Chaperones FACT and Spt6 Restrict H2A.Z from Intragenic Locations. Mol. Cell 58, 1113–1123. 10.1016/j.molcel.2015.03.030. [PubMed: 25959393]

120. Duina AA (2011). Histone Chaperones Spt6 and FACT: Similarities and Differences in Modes of Action at Transcribed Genes. Genet. Res. Int 2011, 625210–12. 10.4061/2011/625210. [PubMed: 22567361]

121. Kurat CF, Yeeles JTP, Patel H, Early A, and Diffley JFX (2017). Chromatin Controls DNA Replication Origin Selection, Lagging-Strand Synthesis, and Replication Fork Rates. Mol. Cell 65, 117–130. 10.1016/j.molcel.2016.11.016. [PubMed: 27989438]

122. Foltman M, Evrin C, De Piccoli G, Jones RC, Edmondson RD, Katou Y, Nakato R, Shirahige K, and Labib K (2013). Eukaryotic replisome components cooperate to process histones during chromosome replication. Cell Rep. 3, 892–904. 10.1016/j.celrep.2013.02.028. [PubMed: 23499444]

123. Gasparian AV, Burkhart CA, Purmal AA, Brodsky L, Pal M, Saranadasa M, Bosykh DA, Commane M, Guryanova OA, Pal S, et al. (2011). Curaxins: Anticancer compounds that simultaneously suppress NF-κB and activate p53 by targeting FACT. Sci. Transl. Med 3, 95ra74–13. 10.1126/scitranslmed.3002530.

124. Yang J, Zhang X, Feng J, Leng H, Li S, Xiao J, Liu S, Xu Z, Xu J, Li D, et al. (2016). The Histone Chaperone FACT Contributes to DNA Replication-Coupled Nucleosome Assembly. Cell Rep. 14, 1128–1141. 10.1016/j.celrep.2015.12.096. [PubMed: 26804921]

125. Appanah R, Lones EC, Aiello U, Libri D, and De Piccoli G (2020). Sen1 Is Recruited to Replication Forks via Ctf4 and Mrc1 and Promotes Genome Stability. Cell Rep. 30, 2094–2105.e9. 10.1016/j.celrep.2020.01.087. [PubMed: 32075754]

126. Köster J, and Rahmann S (2012). Snakemake-a scalable bioinformatics workflow engine. Bioinformatics 28, 2520–2522. 10.1093/bioinformatics/bts480. [PubMed: 22908215]

127. Langmead B, and Salzberg SL (2012). Fast gapped-read alignment with Bowtie 2. Nat. Methods 9, 357–359. 10.1038/nmeth.1923. [PubMed: 22388286]

128. Li H, Handsaker B, Wysoker A, Fennell T, Ruan J, Homer N, Marth G, Abecasis G, and Durbin R; 1000 Genome Project Data Processing Subgroup (2009). The Sequence Alignment/Map format and SAM tools. Bioinformatics 25, 2078–2079. 10.1093/bioinformatics/btp352. [PubMed: 19505943]

129. Ramírez F, Ryan DP, Grüning B, Bhardwaj V, Kilpert F, Richter AS, Heyne S, Dündar F, and Manke T (2016). deepTools2: a next generation web server for deep-sequencing data analysis. Nucleic Acids Res. 44, W160–W165. 10.1093/nar/gkw257. [PubMed: 27079975]

130. Stark R, and Brown G (2011). DiffBind : differential binding analysis of ChIP-Seq peak data.

131. Laughery MF, Hunter T, Brown A, Hoopes J, Ostbye T, Shumaker T, and Wyrick JJ (2015). New Vectors for Simple and Streamlined CRISPR-Cas9 Genome Editing in Saccharomyces cerevisiae. Yeast 32, 711–720. 10.1002/yea.3098. [PubMed: 26305040]

132. Gambus A, Jones RC, Sanchez-Diaz A, Kanemaki M, van Deursen F, Edmondson RD, and Labib K (2006). GINS maintains association of Cdc45 with MCM in replisome progression complexes at eukaryotic DNA replication forks. Nat. Cell Biol 8, 358–366. 10.1038/ncb1382. [PubMed: 16531994]

133. Zhang Y, Liu T, Meyer CA, Eeckhoute J, Johnson DS, Bernstein BE, Nusbaum C, Myers RM, Brown M, Li W, and Liu XS (2008). Model-based analysis of ChIP-Seq (MACS). Genome Biol. 9, R137. 10.1186/gb-2008-9-9-r137. [PubMed: 18798982]

Highlights

- Spt6 has been primarily studied as a histone chaperone important for transcription
- Spt6 mutants exhibit genomic instability, consistent with DNA replication defects
- Spt6 mutants are defective for DNA replication *in vivo*
- The replication defect is likely at the initiation stage, during origin licensing

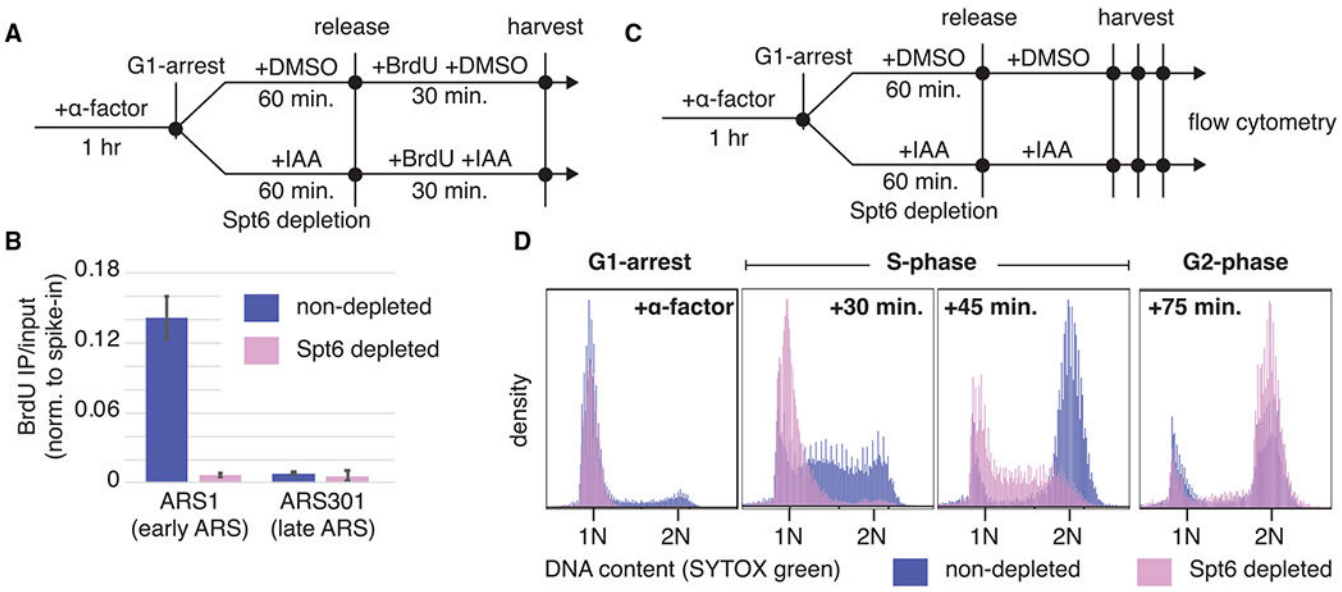

Figure 1. DNA replication defects following Spt6 depletion

(A) Schematic of cell synchronization, Spt6 depletion, and harvesting strategy for the experiment shown in (B).

(B) BrdU-IP-qPCR IP/input (n = 2), data are normalized to 10% BrdU-labeled *S. pombe* genomic DNA. The error bars indicate the standard deviations.

(C) Schematic of cell synchronization, Spt6 depletion, and harvesting strategy for the experiment shown in (D).

(D) Representative flow cytometry analysis of DNA content for samples stained with SYTOX green. Shown is one of two similar replicates.

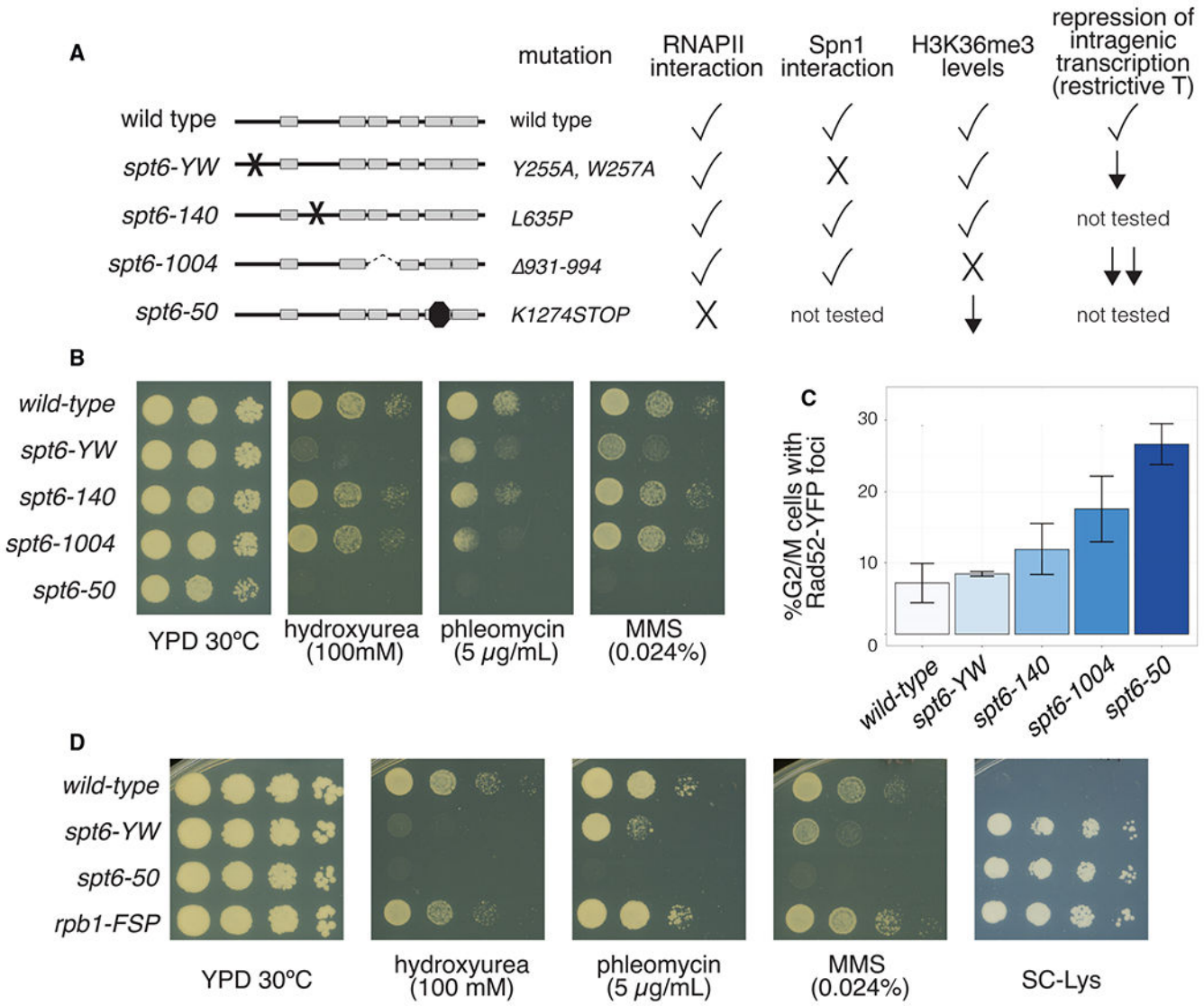

Figure 2. *spt6* mutants exhibit elevated DNA replication stress phenotypes

(A) Schematic of *spt6* mutations. Conserved domains[26] are indicated as gray boxes. An "X" indicates a point mutation, a dashed line indicates a deleted region, and an octagon indicates a nonsense mutation. The amino acid changes caused by each mutation are indicated to the right of the diagram. Additional information for each mutant is in the chart to the right with a check indicating wild-type phenotypes, an X indicating undetectable, and a down arrow indicating a decrease.

(B) Testing of *spt6* mutants for sensitivity to DNA-damaging agents. Strains were serially diluted 10-fold, spotted onto the indicated plates, and incubated at 30°C for 3 days. A representative image is shown; all strains were tested at least three times with similar results.

(C) Quantification of Rad52-YFP foci in G2/M cells. Cells were staged based on cell morphology, and the foci were manually counted. Average values are plotted for at least two replicates (n = 2) and over 500 cells per genotype. The error bars indicate the standard deviations.

(D) Testing of an *rpb1-FSP* mutant for sensitivity to DNA-damaging agents, with *spt6* mutants shown as controls. Strains were serially diluted 10-fold, spotted onto the indicated plates, and incubated at 30°C for 3 days. A representative image is shown; all strains were tested at least three times with similar results.

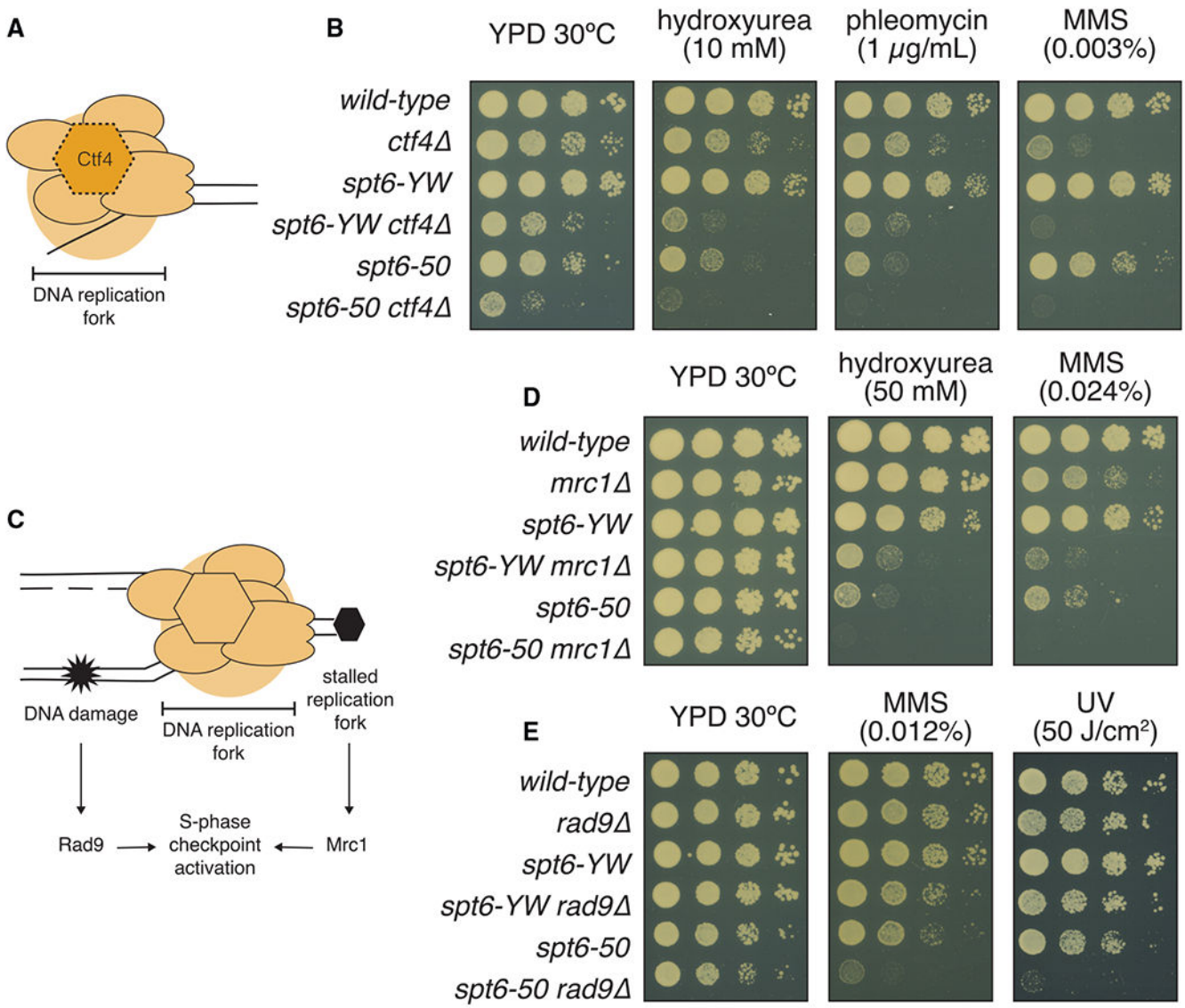

Figure 3. *spt6* mutants have negative genetic interactions with mutations that impair a DNA replication factor and S-phase checkpoint factors

(A and C) Schematic of genetic interactors.

(B, D, and E) Strains were serially diluted 10-fold, plated on the indicated plates, and incubated at 30°C for 3 days. A representative image is shown; all genotypes were tested at least three times (n = 3) with similar results from two independently derived sets of strains.

(A and B) Ctf4 is a non-essential member of the DNA replication fork complex.

(C and D) Mrc1 is an S-phase checkpoint mediator that responds to stalled DNA replication forks.

(C and E) Rad9 is an S-phase checkpoint mediator that responds to DNA damage.

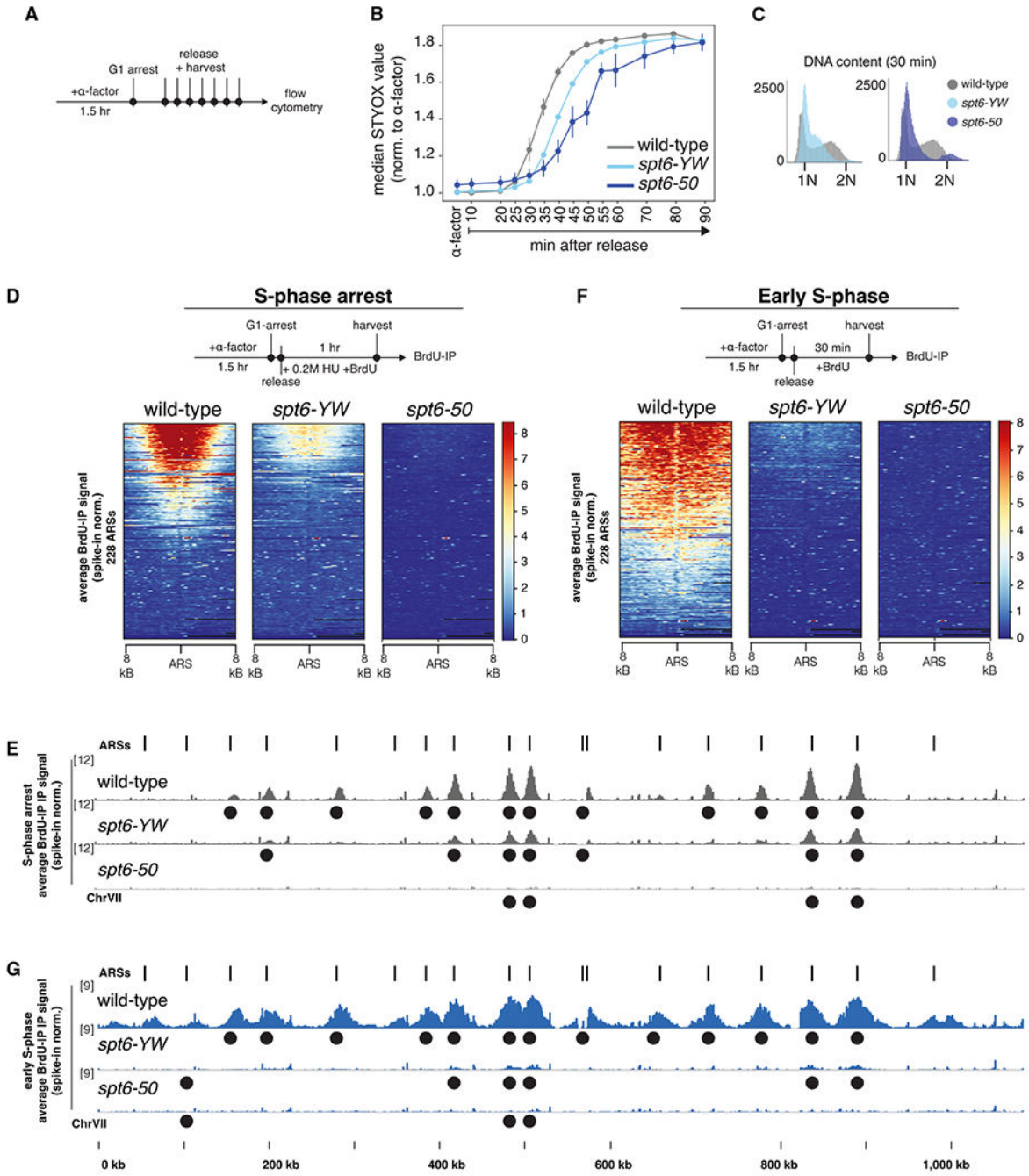

Figure 4. *spt6* mutants have DNA replication defects *in vivo*

(A) Schematic of cell synchronization and harvest strategy for the experiments shown in (B) and (C).

(B) Flow cytometry analysis was performed for wild type (n = 2), *spt6-YW* (n = 2), and *spt6-50* (n = 3). The median fluorescence signal over time was plotted and normalized for the signal in α-factor-arrested cells. Error bars indicate the standard deviations.

(C) A representative flow cytometry histogram of total DNA content for the indicated strains at 30 min following release from α-factor. Median values with standard deviation were plotted versus time.
(D and F) Spike-in normalized BrdU-IP-seq signal at 228 origins (ARSs) in indicated strains and growth conditions. The signal represents the average of biological duplicates (n = 2).
(E and G) Representative genome browser views of *S. cerevisiae* chromosome VII. Previously identified ARSs are indicated by vertical lines above. Black circles represent ARSs called in our peak-calling pipeline. The results for S-phase-arrested cells (gray, E) and early-S-phase cells (blue, G) are shown for biological duplicates.
See also Figure S3.

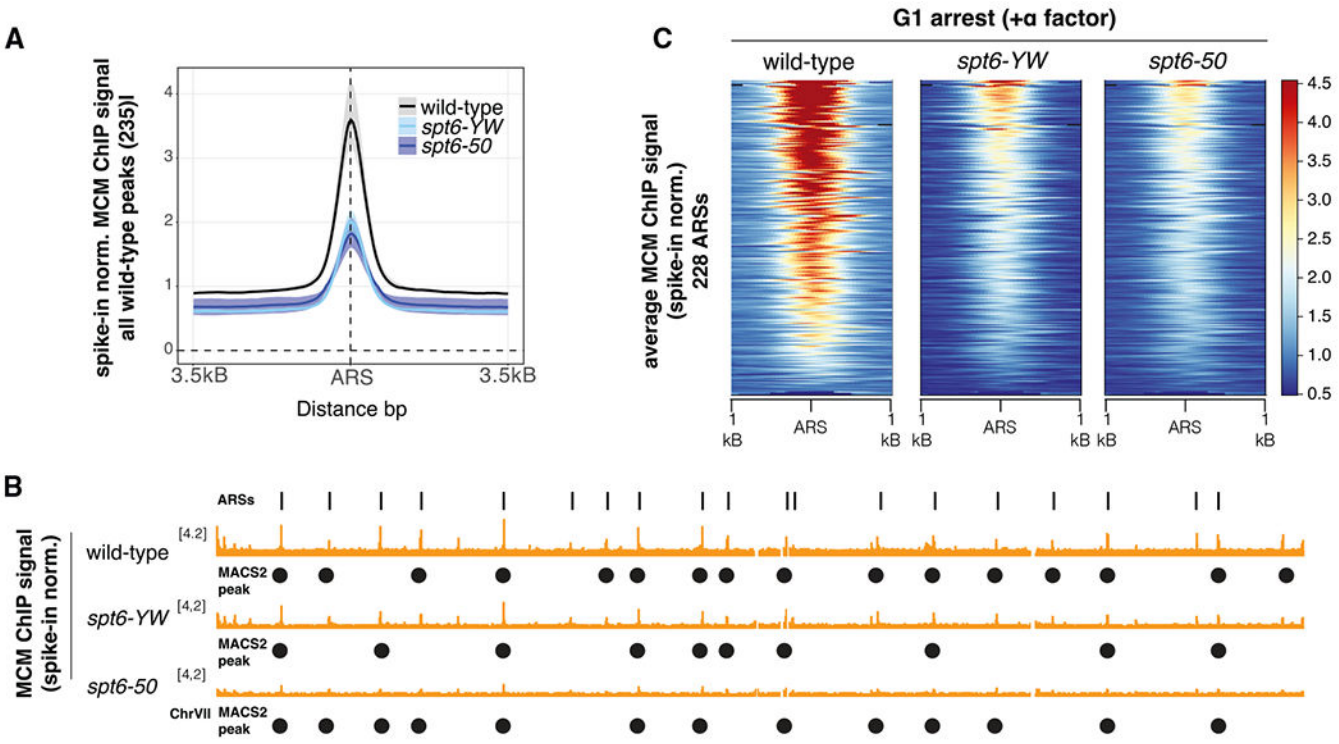

Figure 5. *spt6* mutants have a reduced level of MCM complexes associated with ARSs

(A) Spike-in normalized MCM-ChIP-seq signal at 235 high-confidence wild-type peak regions in indicated strains in α-factor-arrested cells; each line represents the median, and the shading indicates the interquartile range for each strain from experiments done in biological triplicate (n = 3).

(B) A representative genome browser view of *S. cerevisiae* chromosome VII. Previously identified ARSs are indicated by vertical lines above the track. Black circles represent origins called in our peak-calling pipeline.

(C) Spike-in normalized MCM-ChIP-seq signal at 228 origins in indicated strains in α-factor-arrested cells, average signal across biological triplicate samples. See also Figure S4.

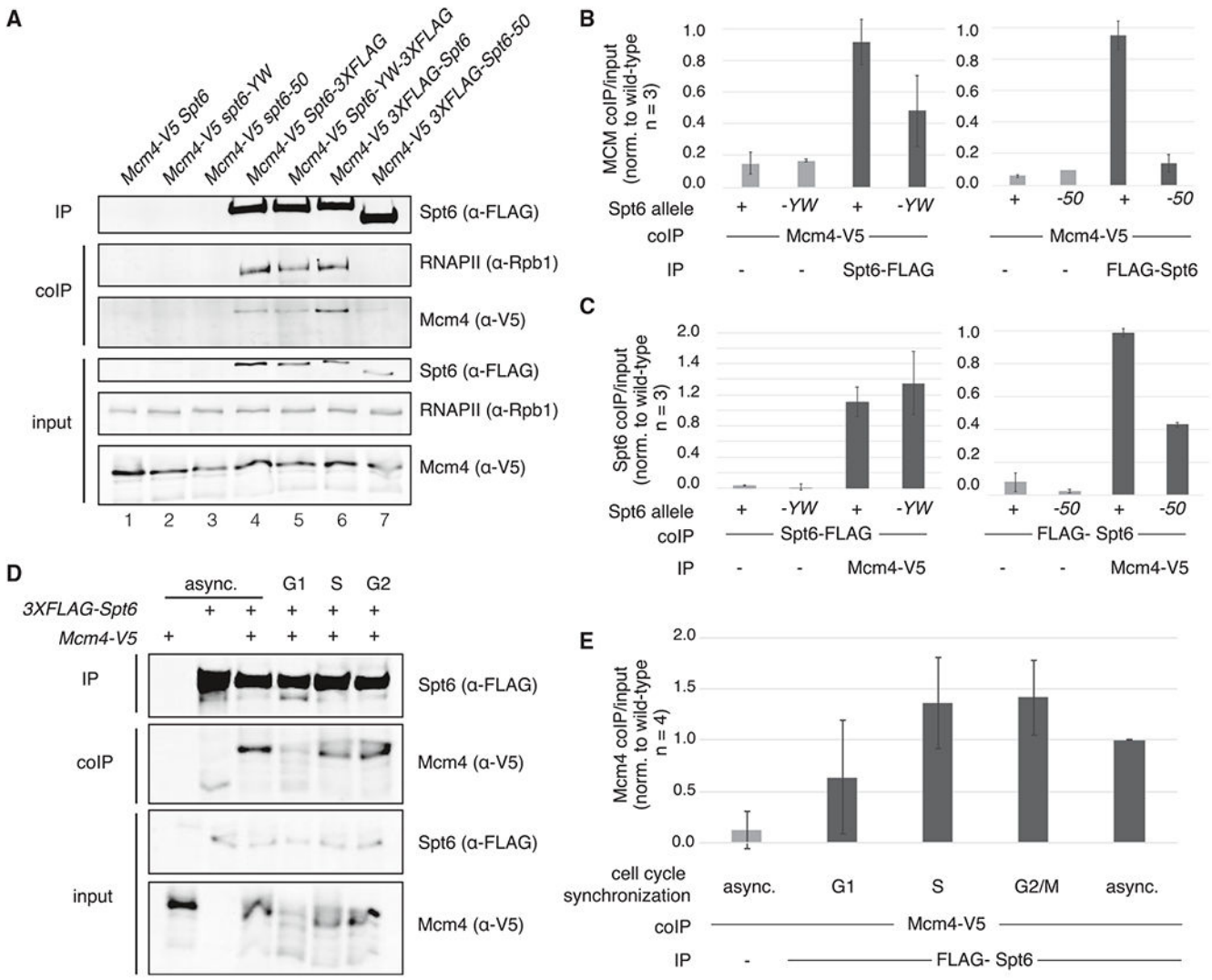

Figure 6. Spt6 may physically interact with the MCM complex

(A) A representative western blot showing the immunoprecipitation of either wild-type or mutant Spt6 and the co-immunoprecipitation (coIP) of Rpb1 and Mcm4.

(B) Quantification of three independent coIP experiments as shown in (A) (n = 3). The error bars represent the standard deviations.

(C) Quantification of three independent coIP experiments in which Mcm4-V5 was immunoprecipitated and wild-type or mutant Spt6 coIP was assayed (n = 3). The error bars represent the standard deviations.

(D) A representative western blot of Spt6 immunoprecipitation in synchronized cells: G1 (α-factor arrest), S (0.2 M HU arrest), and G2 (15 μg/mL nocodazole arrest).

(E) Quantification of four independent coIP experiments shown in (D) (n = 4). The error bars represent the standard deviations.

See also Figure S5.

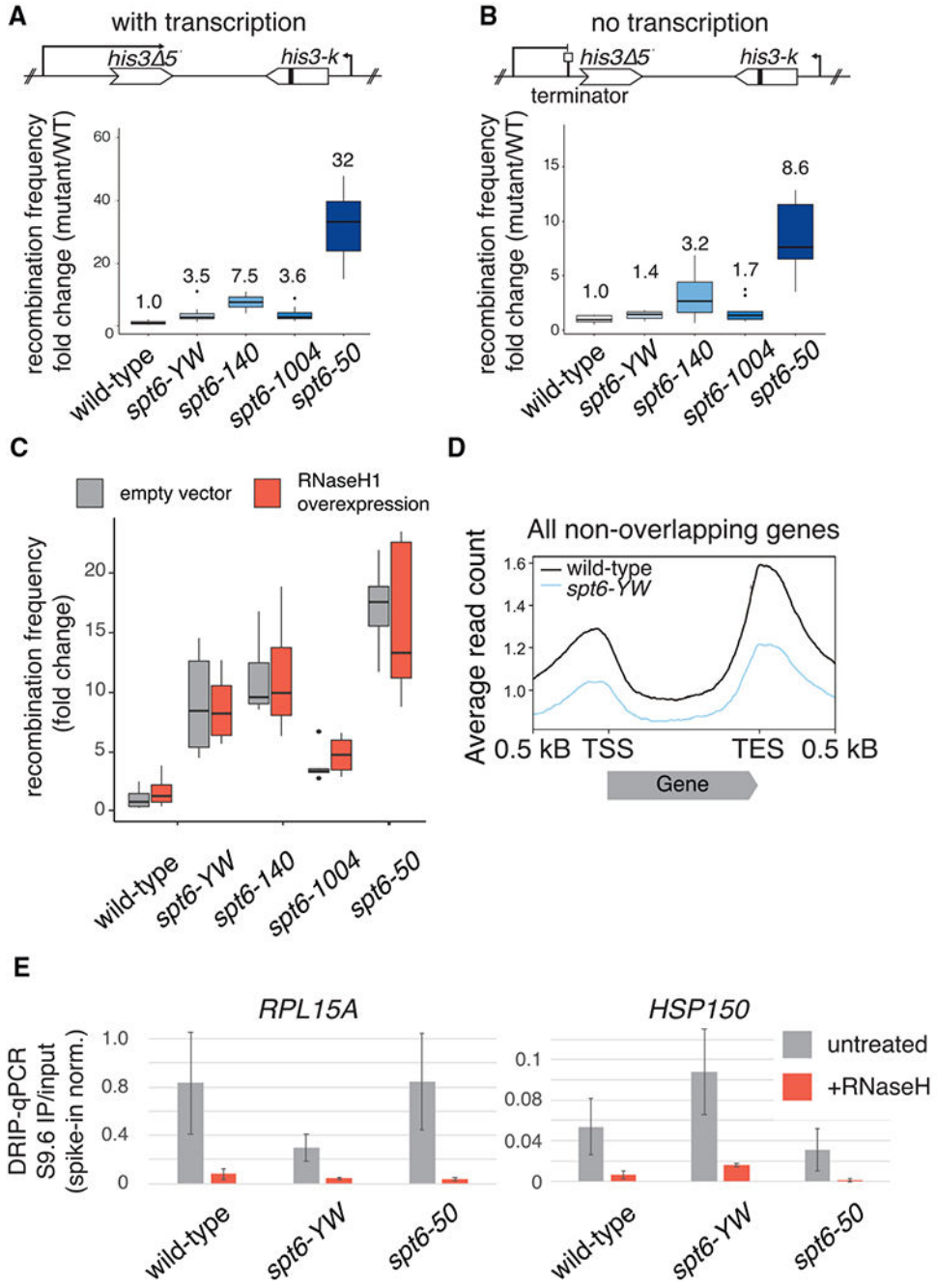

Figure 7. Transcription contributes to *spt6* genome instability

(A) Quantification of an inverted repeat recombination assay.[56] Two independently derived strains and six independent colonies were assayed per genotype (n = 12). The values represent the average across all samples of a particular genotype. Wild-type values were averaged across replicates.

(B) Quantification of inverted repeat recombination assay in the absence of transcription; conducted as in (B).

(C) Quantification of an inverted repeat recombination assay, as in (A) except that strains were grown in SC-Trp media and *RNH1* transcription from plasmid pKW26 was induced by overnight treatment with estrodiol. Two independently derived strains were tested per condition (n = 2).

(D) Metagene profile of all *S. cerevisiae* non-overlapping genes scaled to their respective transcription start site (TSS) and transcription end site (TES) from DRIP-seq. Data represent the average of two biological replicates (n = 2).

(E) Spike-in normalized DRIP-qPCR data IP/input for two known R-loop-containing mRNA genes: *RPL15A* and *HSP150*. The average value for biological duplicates is shown (n = 2). The error bars show the standard deviations.

KEY RESOURCES TABLE

REAGENT or RESOURCE	SOURCE	IDENTIFIER
Antibodies		
Anti-V5	Invitrogen	R960-25; RRID: AB_2556564
ANTI-FLAG M2 Affinity Gel	Sigma	A2220; RRID: 10063035
ANTI-FLAG M2	Sigma	F3165; RRID: 259529
Anti-RNA Polymerase II CTD	MilliporeSigma	clone 8WG16; RRID: 1977470
Purified Mouse Anti-BrdU	BD Pharmingen	555627; RRID: 395993
S9.6	provided by Koshland lab	N/A
MCM antisera UM174	provided by Bell lab	N/A
IRDye 800 Goat anti-Mouse IgG Secondary	Licor	925032210; RRID: 621842
Chemicals, peptides, and recombinant proteins		
alpha-factor	BioSynthesis custom peptide: WHWLQLKPGQPMY	N/A
Pronase from *Streptomyces griseus*	Roche	10165921001
RnaseA Solution	Sigma	R6148
Proteinase K, recombinant PCR grade	Roche	3115801001
SYTOX Green nucleic acid stain	Invitrogen	57020
Hydroxyurea	Sigma	H8627
Nocodazole	Sigma	M1404
Methyl methanesulfonate (MMS)	Sigma	M4016
Phleomycin from *Streptomyces verticillus*	Sigma	P9564
3-Indoleacetic acid (IAA)	Sigma	12886
RnaseH	NEB	M0297L
AccI	NEB	R0161S
EcoRV	NEB	R3195S
NcoI	NEB	R3193S
HaeIII	NEB	R0108S
BsrG1	NEB	R3575S
SigmaFAST protease inhibitor cocktail tablets	Sigma	S8820-20TAB
RNaseA/T1 Mix	Thermo	EN0551
Benzonase	Sigma	E1014-5KU
Dynabeads Protein G	Invitrogen	10004D
Dynabeads Protein A	Invitorgen	10002D
Critical commercial assays		
Genomic-tip 100/G	Qiagen	10243
Genomic DNA Buffer Set	Qiagen	19060
GeneRead DNA Library I Core Kit	Qiagen	180434
Deposited data		
RNAPII ChIP-seq	[60]	GEO: GSE160821

REAGENT or RESOURCE	SOURCE	IDENTIFIER
DRIP-seq	This study	GEO: GSE201633
BrdU-IP-seq	This study	GEO: GSE201632
MCM ChIP-seq	This study	GEO: GSE221913
Experimental models: Organisms/strains		
Listed as Table S2.	N/A	N/A
Oligonucleotides		
qPCR ARS1 F: AATGACCCGATTCTTGCTAG	This study	N/A
qPCR ARS1 R: GGATACGGAGAGAGGTATGT	This study	N/A
qPCR ARS301 F: GGATCTAGGGTTTTATGCCTT	This study	N/A
qPCR ARS301 R: TATCTTCTGGTGTCTCGTCC	This study	N/A
qPCR HSP150 F: CGGTAACTTGGCTATTGGTGA	Wahba et al.[95]	N/A
qPCR HSP150 R: CGATAGCTTCCAAGTGGACTG	Wahba et al.[95]	N/A
qPCR RPL15A F: ACC GCT GAA GAA AGA GTT GG	Wahba et al.[95]	N/A
qPCR RPL15A R: TGT TGA GGG TCG ACC AAG AT	Wahba et al.[95]	N/A
Additional oligos used for strain construction are listed in Table S2.	N/A	N/A
Recombinant DNA		
pKW26	This study	N/A
Software and algorithms		
Original code	This study	https://github.com/winston-lab; https://doi.org/10.5281/zenodo.7644131
Snakemake	Köster and Rahmann[126]	https://snakemake.readthedocs.io/en/stable/
Bowtie2	Langmead and Salzberg[127]	http://bowtie-bio.sourceforge.net/bowtie2/index.shtml
Cutadapt	N/A	https://cutadapt.readthedocs.io/en/stable/
Samtools	Li et al.[128]	http://samtools.sourceforge.net/
Bedtools	N/A	https://bedtools.readthedocs.io/en/latest/
Deeptools	Ramírez et al.[129]	https://deeptools.readthedocs.io/en/develop/
DiffBind	Stark and Brown[130]	http://bioconductor.org/packages/release/bioc/html/DiffBind.html
FlowCytometryTools	N/A	https://eyurtsev.github.io/FlowCytometryTools/
ImageStudioLite	Licor	https://www.licor.com/bio/image-studio-lite/
Microsoft Excel	N/A	N/A